



Schweizerische Eidgenossenschaft
Confédération suisse
Confederazione Svizzera
Confederaziun svizra

Swiss Confederation

Federal Department of Home Affairs FDHA
Federal Office of Meteorology and Climatology MeteoSwiss

MeteoSwiss

Technical Report MeteoSwiss No. 270

Exploring quantile mapping as a tool to produce user-tailored climate scenarios for Switzerland

Feigenwinter I., Kotlarski S., Casanueva A., Fischer A.M., Schwierz C., Liniger M. A.



ISSN: 2296-0058

Technical Report MeteoSwiss No. 270

Exploring quantile mapping as a tool to produce user-tailored climate scenarios for Switzerland

Feigenwinter I., Kotlarski S., Casanueva A., Fischer A.M., Schwierz C., Liniger M. A.

Recommended citation:

Feigenwinter I, Kotlarski S, Casanueva A, Fischer AM, Schwierz C, Liniger MA, 2018: Exploring quantile mapping as a tool to produce user-tailored climate scenarios for Switzerland, *Technical Report MeteoSwiss*, **270**, 44 pp.

Editor:

Federal Office of Meteorology and Climatology, MeteoSwiss, © 2018

MeteoSwiss

Operation Center 1
CH-8044 Zürich-Flughafen
T +41 58 460 99 99
www.meteoschweiz.ch

Abstract

In the context of the upcoming CH2018 Swiss climate scenarios, empirical quantile mapping (QM) is employed to bias-correct and to downscale raw climate model output enabling the production of user-tailored data products that are directly applicable in climate impact research. We here present the overall CH2018 QM approach as well as exemplary results. The approach consists of three different QM setups that target three different spatial scales. All setups produce transient time series (1981-2099) of several meteorological variables at daily resolution and for all climate model chains considered in CH2018.

The evaluation of QM yields a satisfactory performance in the historical reference period. Systematic climate model biases of seasonally averaged quantities are largely removed, and spatial climate variability at climatological time scales is properly represented by the QM data. As a consequence of removing intensity-dependent climate model biases, QM can slightly modify the raw models' climate change signals. But the overall consistency with the raw model output and, hence, with further CH2018 products is maintained.

The QM-derived scenario-data products can ultimately be employed by climate impact studies over the Swiss terrain but, at the same time, are subject to a number of caveats and limitations. These need to be properly assessed by users for each specific application.

Zusammenfassung Riassunto Résumé

Die neueste Generation Schweizer Klimaszenarien CH2018 verwendet eine empirisch-statistische Methode, um grob aufgelöste und fehlerbehaftete Klimamodelldaten zu korrigieren und auf lokale Skalen anzupassen: Quantile Mapping (QM). Die resultierenden QM-basierten Szenario-Produkte sind damit direkt in einer Vielzahl von Klimafolgenstudien anwendbar. Der vorliegende Bericht gibt einen Überblick über die in CH2018 verwendete QM Implementation und präsentiert beispielhaft Ergebnisse. Die Implementation besteht aus drei verschiedenen QM Varianten, die unterschiedliche räumliche Skalen anvisieren. Alle Varianten liefern transiente Zeitreihen (1981-2099) mehrerer meteorologischer Variablen in täglicher Auflösung und für alle in CH2018 verwendeten Klimamodellketten.

Die Validierung des verwendeten QM Ansatzes in einer historischen Referenzperiode zeigt eine effektive und zufriedenstellende Korrektur systematischer mittlerer Modellfehler. Auch die räumliche Klimavariabilität wird durch die QM-basierten Produkte gut abgebildet. Zukünftige Klimaänderungssignale der rohen, unprozessierten Klimamodelldaten können durch Anwendung von QM zu einem gewissen Grad verändert werden. Dies beruht in erster Linie auf der erwünschten Berücksichtigung intensitätsabhängiger Modellfehler durch QM. Prinzipiell wird aber eine Konsistenz mit den Änderungssignalen der rohen Klimamodelldaten und damit auch mit weiteren CH2018 Produkten bewahrt.

Die QM-basierten Szenario-Produkte sind direkt in Klimafolgenstudien in der Schweiz anwendbar. Es sind bei der Anwendung jedoch auch eine Reihe von Limitierungen und nicht zulässiger Analysen zu beachten. Diese müssen von Nutzern vor der Verwendung der QM Daten eingeschätzt und entsprechend berücksichtigt werden.

Contents

Abstract	V
Zusammenfassung Riassunto Résumé	VI
1 Introduction	8
2 Data and Methods	10
2.1 Quantile Mapping	10
2.2 Implementation at MeteoSwiss	11
2.3 Climate model data	13
2.4 QM to stations (Setup A)	14
2.5 QM on RCM grid (Setup B)	15
2.6 QM to high-resolution grid (Setup C)	16
2.7 Multi-model combination and pattern scaling	16
2.8 Calculation of temperature indices	17
3 Results	18
3.1 QM evaluation: Individual models	18
3.1.1 QM to stations (Setup A)	18
3.1.2 QM on RCM grid (Setup B)	21
3.1.3 QM to high-resolution grid (Setup C)	23
3.2 QM evaluation: Model ensemble	26
3.3 QM scenarios	29
4 Limitations	36
5 Summary and Conclusions	39
Acknowledgment	40
References	40

1 Introduction

Climate model data are nowadays used in various fields of application, including the assessment of future climate change impacts at local to regional scales. Such efforts often require a higher spatial resolution than currently provided by global or regional climate models (GCMs, RCMs). Furthermore, climate model data can be subject to systematic biases (e.g. Kotlarski, et al. 2014), which often prevents the direct use of raw climate model output in subsequent applications.

As a response to these challenges and in order to translate coarsely resolved and potentially biased climate model output into forcing data that are directly applicable to impact models, a large number of statistical downscaling (SD) and bias correction (BC) approaches have been developed over the recent decades. Comprehensive overviews are provided by e.g. Wilby and Wigley (2000), Fowler et al. (2007), Maraun et al. (2010), Wilby and Fowler (2011), or Maraun and Widmann (2018). **Figure 1** lists some of the most common approaches. For producing the previous widely-used CH2011 Swiss Climate Change Scenarios (CH2011 2011) the well-established delta change method was employed. Here, a climate change signal (*delta*) is computed by comparing raw climate model output for a future scenario and a historical reference period. In a second step, the delta is used to scale observational time series in either an additive or a multiplicative manner, yielding series for a future scenario period that reflect the spatial and temporal scale of the underlying observations.

The local daily product of the CH2011 scenarios relied on a specific implementation of the delta change method (Bosshard et al. 2011) and provided the mean annual cycle of temperature and precipitation changes for 188 and 565 Swiss stations, respectively. Advantages of this approach are, among others, its easy implementation and robustness, the possibility to obtain spatially consistent

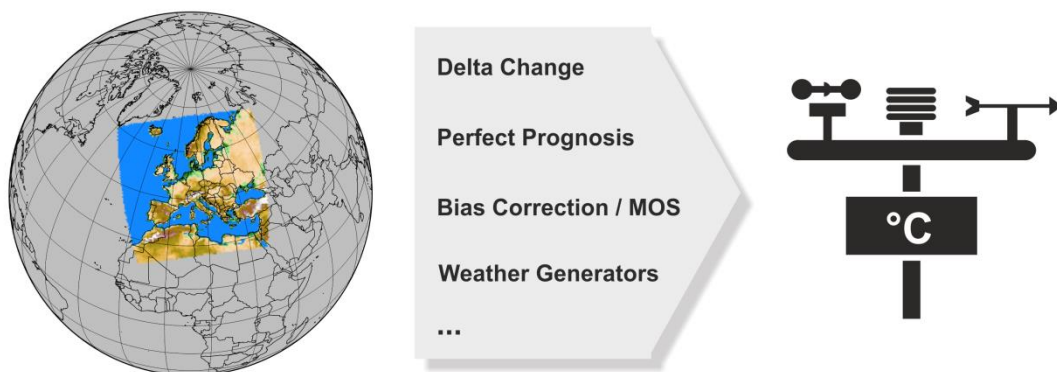


Figure 1 Some examples of available downscaling methods to translate (global or regional) climate model output to local scales.

multi-site scenario series (based on the observed record at multiple sites) and its inter-variable consistency (based on the observational record of several variables at a given site). However, delta change is subject to a number of assumptions and limitations. The mean climate change signal is assumed to be valid for all distributional quantiles (i.e. to apply for both mean and extreme conditions), and systematic model biases are implicitly assumed to be stationary in the long term (i.e. to apply for both the historical reference and the future scenario period). Furthermore, the temporal variability of the constructed future time series reflects the variability of the observational period and potential future changes in temporal climate variability are neglected. Last but not least, delta change is by definition a time slice-based approach and does not provide information for times between the end of the reference and the start of the scenario period. Such transient information would have to be produced by further gap-filling methods.

The next generation of Swiss Climate Change Scenarios to be released in 2018 (*CH2018*; <http://www.climate-scenarios.ch>) aims at improving on some of these caveats and, for the case of site-specific local scenarios at daily resolution, will replace delta change by a *bias correction* approach. Here, simulated model output is corrected towards an observational reference and systematic model biases are partly removed. In a climate change context, the so-called *correction function* (or *transfer function*), established in the historical calibration period, can then be applied to the simulated future time series in order to produce bias-corrected scenario time series (**Figure 2**).

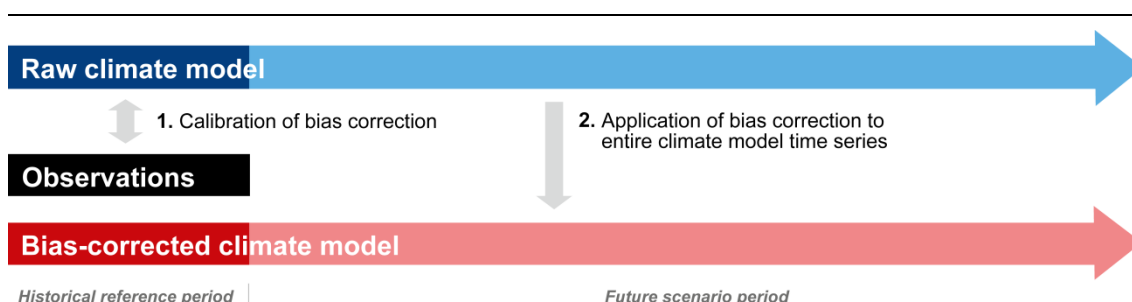


Figure 2: Overview on the bias correction approach: a bias correction function is calibrated by comparing raw climate model output to observations in a common historical reference period. The calibrated correction function is then applied to the entire raw model output in order to produce a bias-corrected time series out into the future scenario period.

The bias correction method employed in the frame of CH2018 is *Quantile Mapping* (QM). During the last years QM has become increasingly popular and is widely used for both correcting systematic biases of climate model simulations and for bridging the scale gap between coarse resolution climate model output and the site scale. The specific QM implementation used is a variant of *Empirical Quantile Mapping* and originates from the works of Rajczak et al. (2016a) and Ivanov and Kotlarski (2017). The present report is concerned with exploring, presenting and discussing details of this implementation and thereby serves as a basic reference and background document for the downscaled CH2018 products. The specific objectives of this report are:

- (1) To present the QM variant employed within CH2018 and its specific implementation at the Swiss Federal Office of Meteorology and Climatology (MeteoSwiss).

- (2) To evaluate the performance of the QM implementation in the historical reference climate.
- (3) To present an exemplary overview of the results obtained in terms of future climate change over Switzerland as represented by the QM-based scenario products.
- (4) To outline potential caveats and limitations of the QM-based products that need to be taken into account by users.

2 Data and Methods

2.1 Quantile Mapping

Quantile Mapping (QM) originates from the empirical transformation of Panofsky and Brier (1968) and, if employed in a climate modelling context, corrects for biases in the distribution of a simulated variable by comparing raw model output against an observational distribution of the same variable. Simulated and observed distributions are approximately matched by establishing a quantile-dependent correction function that translates simulated quantiles into their observed counterparts (**Figure 3**). This function is afterwards used to translate a transient simulated time series into a bias-corrected series. The implicit assumption of QM is that a climate model can accurately project ranked categories of the variable of interest, i.e. quantiles, but not its actual values (Déqué et al. 2007). Simulated and observed quantiles can either be based on the full empirical distribution (non-parametric implementation; e.g. Déqué et al. 2007, Themessl et al. 2012) or on a fitted theoretical distribution (parametric implementation, e.g. Piani et al. 2010).

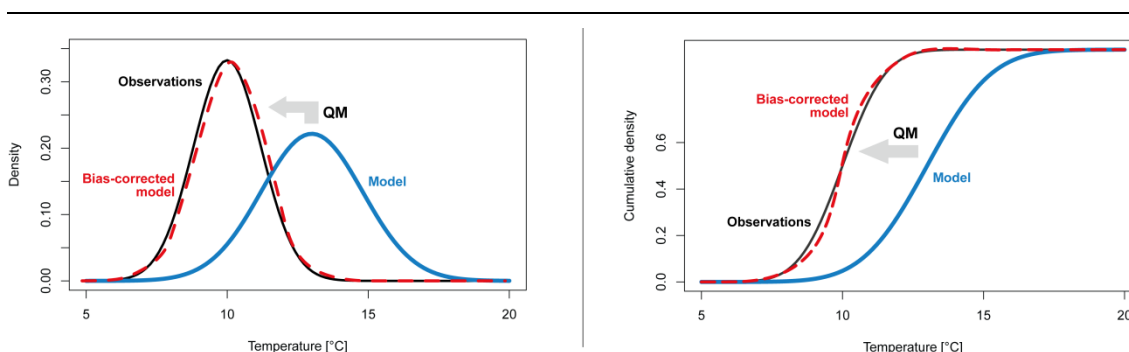


Figure 3: The nature of QM: A biased simulated distribution (blue) is corrected towards an observed distribution (black). In the example shown the raw simulated distribution is subject to both a bias of the mean and a bias in variance. The resulting bias-corrected distribution (dashed red) approximates the observed one but is typically not identical to it (e.g. due to the sampling uncertainty during the calibration of the correction function or details of the specific QM implementation). Left panel: Example based on the probability density function (PDF). Right panel: example based on the cumulative distribution function (CDF).

QM as such is a bias correction method but can implicitly include a downscaling component. If the observed reference data against which the simulated distribution is matched reflects a higher spatial scale than the underlying climate model data the bias-corrected distribution is, in principle, valid for that higher spatial scale. A typical example is the mapping of a simulated grid-cell based distribution (reflecting an area average over the respective climate model grid cell) onto a distribution measured at a specific weather station. Note, however, that certain aspects of the bias-corrected time series might still reflect the spatial scale of the underlying climate model. As such, the additional downscaling component involves specific assumptions and comes along with potential risks and limitations (Maraun 2013, Maraun 2016, Maraun et al. 2017).

A large number of recent studies applied QM in a downscaling context and documented the method's general applicability and performance, which is often similar or superior to other statistical downscaling approaches (Boé et al. 2007, Themessl et al. 2011; Gudmundsson et al. 2012; Themessl et al. 2012, Gutiérrez et al. 2018). For the case of Switzerland Rajczak et al. (2016a), Rajczak et al. (2016b) and Ivanov and Kotlarski (2017) applied and extensively validated QM for a large number of MeteoSwiss stations and for several meteorological variables that are also targeted in the context of CH2018.

2.2 Implementation at MeteoSwiss

The QM variant employed in the context of CH2018 is based on the work of Rajczak et al. (2016a), Rajczak et al. (2016b) and Ivanov and Kotlarski (2017; method *linear_add*) and has been implemented in the *R Software Environment for Statistical Computing and Graphics* (<https://www.r-project.org>). The Climate Data Operators (CDOs; <https://code.mpimet.mpg.de/projects/cdo>) were used for further processing and analysis steps. Most parts of the QM code were run on the *Piz Kesch* supercomputer at the Swiss National Supercomputing Centre CSCS. The same QM variant has recently also been used in a CH2011 extension that provides bias-corrected scenarios for stations that are consistent with the delta change-based CH2011 products in terms of the underlying climate model chains Kotlarski et al. (2017). Furthermore, an almost identical methodology has also been applied in a similar QM implementation to long-range weather forecasts over the Alps. The validation based on a large sample of 20 years of forecasts showed a good performance in bias removal also in this application (Monhart et al., 2018).

The QM implementation is based on the 99 empirical percentiles (1st to 99th percentile) of the daily time series and an additive quantile-based correction function that translates simulated quantiles into their observed counterparts. The correction function in-between the 99 empirical percentiles is linearly interpolated. Values beyond the 1st and the 99th percentile, and in particular new extremes in the scenario time series, are corrected according to the correction function of the 1st and 99th percentile, respectively. In order to account for seasonally varying bias characteristics the correction function itself is determined separately for each day-of-the-year (DOY) with a moving 91-day window. For the case of precipitation, a wet-day threshold of 0.1 mm/day is considered and an additional frequency adaptation is implemented (e.g. Themessl et al. 2012). This procedure is necessary in the (few) cases where, for a given DOY, the simulated wet-day frequency is smaller than the observed one and additional wet days have to be included in the corrected series in order to match simulated and ob-

served wet-day frequencies. The dry days in the original model output that need to be replaced by wet days are chosen by a random number generator. The same is true for the precipitation amount on these newly introduced wet days, which is randomly drawn from the observed wet day distribution. For cases where the simulated wet-day frequency is larger than the observed one, QM implicitly corrects a biased wet day frequency and no separate frequency adaptation is required.

The calibration period of the correction function is 1981–2010 (except for the QM on RCM grid setup which uses 1981-2008; see below). All simulated quantiles, including those of the future scenario time series, are estimated applying the correction function calibrated in this period. The resulting bias-corrected time series is a transient daily series for the entire simulated period 1981–2099 (see **Figure 2**).

Within CH2018, QM is applied to three different target scales: (A) To the station scale, (B) on the RCM grid, and (C) to high-resolution 2 km grid covering the Swiss domain. **Table 1** gives an overview on these different setups and the data involved. Further details are provided in Sections 2.4 to 2.6. Setup A uses station time series as observational reference, while setups B and C employ gridded products derived from observations. Setup B represents a mere bias correction (spatial scale of the simulations and of the observational reference are identical), while setups A and C additionally involve a downscaling component (RCM grid to stations and RCM grid to 2km grid, respectively). The meteorological variables considered depend on the QM setup, but the three temperature variables (tas, tasmin, tasmax) and precipitation (pr) are covered in all three cases. Setup A (QM to stations) is the primary product provided to climate scenario users.

Table 1: Overview on the three different QM setups. See Sections 2.4 to 2.6 for further details. Meteorological variables for which QM is carried out are: daily mean temperature (tas), daily minimum temperature (tasmin), daily maximum temperature (tasmax), daily precipitation sum (pr), daily mean wind speed (sfcWind), daily mean relative humidity (hurs) and daily mean global radiation (rsds). The CH2018 domain refers to the combined domain of all five CH2018 regions (see CH2018 Technical Report).

	QM setup	Observational data	Model data	Calibration period	QM period	Variables
A	QM to stations	MeteoSwiss daily station time series	Raw RCM data for grid cell that is overlying the station location	1981-2010	1981-2099	tas, tasmin, tasmax, pr, sfcWind, hurs, rsds
B	QM on RCM grid	MeteoSwiss daily 2 km (TabsD, TminD, TmaxD, RhiresD) and further observational grids regridded to RCM resolution over the CH2018 domain	Raw RCM data (all grid cells of CH2018 domain)	1981-2008	1981-2099	tas, tasmin, tasmax, pr
C	QM to high-resolution grid	MeteoSwiss daily 2 km observational grids (TabsD, TminD, TmaxD, RhiresD)	RCM data interpolated to 2 km resolution	1981-2010	1981-2099	tas, tasmin, tasmax, pr

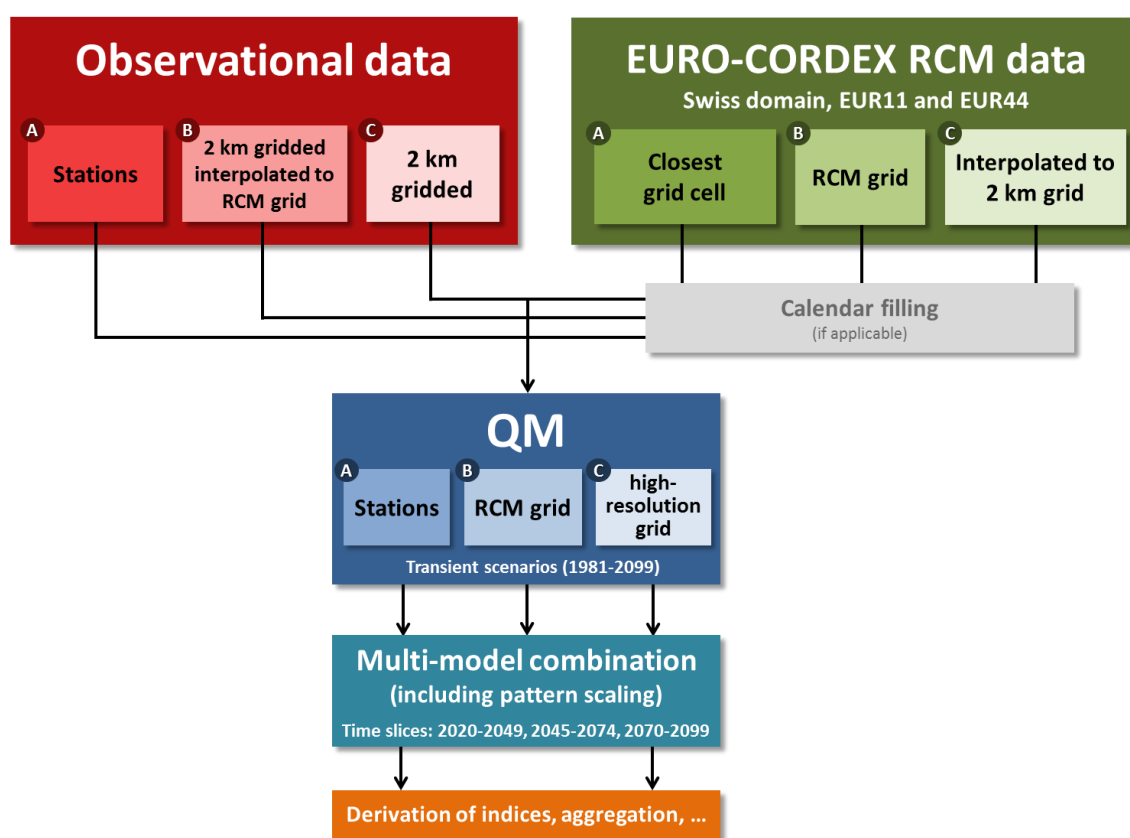


Figure 4: Overview on workflow and data processing.

Figure 4 presents a schematic overview on the internal data processing and the resulting QM products. Prior to QM, the simulated data of RCMs that internally use a 360- or 365-days calendar are converted to a Gregorian calendar by randomly filling in missing values. For a given GCM-RCM chain these random dates are identical for all cases, ensuring full temporal consistency between the QM setups and the individual variables within one setup. After the data have been quantile-mapped and transient scenarios from 1981-2099 have been produced, a multi-model combination including temporal pattern scaling is applied to get a complete model ensemble (see below and the CH2018 technical report for further details). These data are used, for instance, to calculate ensemble median climate change signals and to derive further threshold indices.

2.3 Climate model data

The climate model data used in CH2018 originate from the EURO-CORDEX initiative (Jacob et al. 2014, Kotlarski, et al. 2014) which provides RCM projections until the end of the 21st Century on a 12 km (EUR-11) and a 50 km grid (EUR-44) covering the entire European continent plus adjacent regions. Three different greenhouse gas emission scenarios are covered (*Representative Concentration Pathways* RCP2.6, RCP4.5 and RCP8.5; Moss et al. 2010). In CH2018 only the GCM-driven EURO-CORDEX experiments are considered, i.e. the reanalysis-driven evaluation runs are not analyzed.

For the present report all simulations of the CH2018 model freeze 2.0 have been used. This is not necessarily the final set of model simulations considered in CH2018 as updates of the RCM ensemble might be introduced at a later stage. Freeze 2.0 includes the GCM-driven EURO-CORDEX experiments available in summer 2017 with the exception of a few individual simulations that are disregarded due to substantial simulation shortcomings. Furthermore, data for several individual RCMs have been spatially filtered due to apparent shortcomings in the simulated spatial climate variability. See the CH2018 freeze 2.0 documentation available on http://www.ch2018.ch/wp-content/uploads/2017/07/CH2018_model_ensemble.pdf for further details. The total number of simulations considered (summed up over all RCPs) is 81. These experiments were carried out by 26 different GCM-RCM model chains that combine 10 driving GCMs with 10 different RCMs. Note that, as some experiments do not provide data for all variables, the finally available number of simulations depends on the specific variable considered. While for daily mean temperature and precipitation all 81 experiments are available, the set for further auxiliary variables is smaller and, for the most extreme case of relative humidity, covers 57 simulations only.

Before applying QM, all raw simulation data have been post-processed and brought to a common form consisting of daily fields from 1971 to 2099 on one of the standard grids (EUR-11 or EUR-44). Data of RCMs that internally use a 360- or 365-days calendar were converted to a Gregorian calendar by randomly filling in missing values (see above). Several model chains include additional missing values at a few time steps due to missing raw RCM data at the very beginning or at the end of the respective control and scenario simulations. Furthermore, as the focus region of CH2018 is Switzerland and to increase computational performance, a Swiss mask has been applied to the European-scale EUR-11 and EUR-44 grids, resulting in reduced grids covering the area of Switzerland plus neighboring regions only. Depending on the resolution this reduced grid comprises 768 (EUR-11) or 48 (EUR-44) grid cells in total, defined by a 36x24 or 9x6 rectangle, respectively. With respect to the full EUR-11 (424x412 grid cells) and EUR-44 (106x103 grid cells) domains these rectangles are located at positions [181:216,169:192] and [46:54,43:48], respectively. The data format of both the original EURO-CORDEX data and of the post-processed CH2018 versions is the *Network Common Data Form* (NetCDF; <https://www.unidata.ucar.edu/software/netcdf>).

2.4 QM to stations (Setup A)

For QM to the station scale (setup A; see **Figure 4**) the closest grid cell of the model data provides the simulated input series. The observational data consists of station-based time series obtained from the MeteoSwiss Data Warehouse (DWH). Two different station sets are considered:

The *full set* (**Figure 5**, small panels) covers all stations for which transient QM-based scenarios will be provided in the context of CH2018. It comprises all Swiss stations for which daily data are available during at least 83% of the entire calibration period 1981-2010 (25 out of 30 years) and during at least 83% of the time for each individual DOY. The number of stations in the full set depends on the specific meteorological variable considered and varies from 59 (global radiation) to 399 (precipitation).

The *illustrative set* (**Figure 5**, lower right panel) is a subset of the full set. It is used to present the main results of the station-based scenarios in both this report and in the CH2018 Technical Report. It consists of a basic set of 58 stations at which all seven meteorological variables considered (see

Table 1) are available (red markers). Depending on the specific variable, further stations of the climatologically important *Swiss National Basic Climatological Network (NBCN)* are added if available (blue markers). The same criterion for data availability as in the full set is employed.

Setup A constitutes the primary CH2018 scenario product that is provided to users in the impacts community.

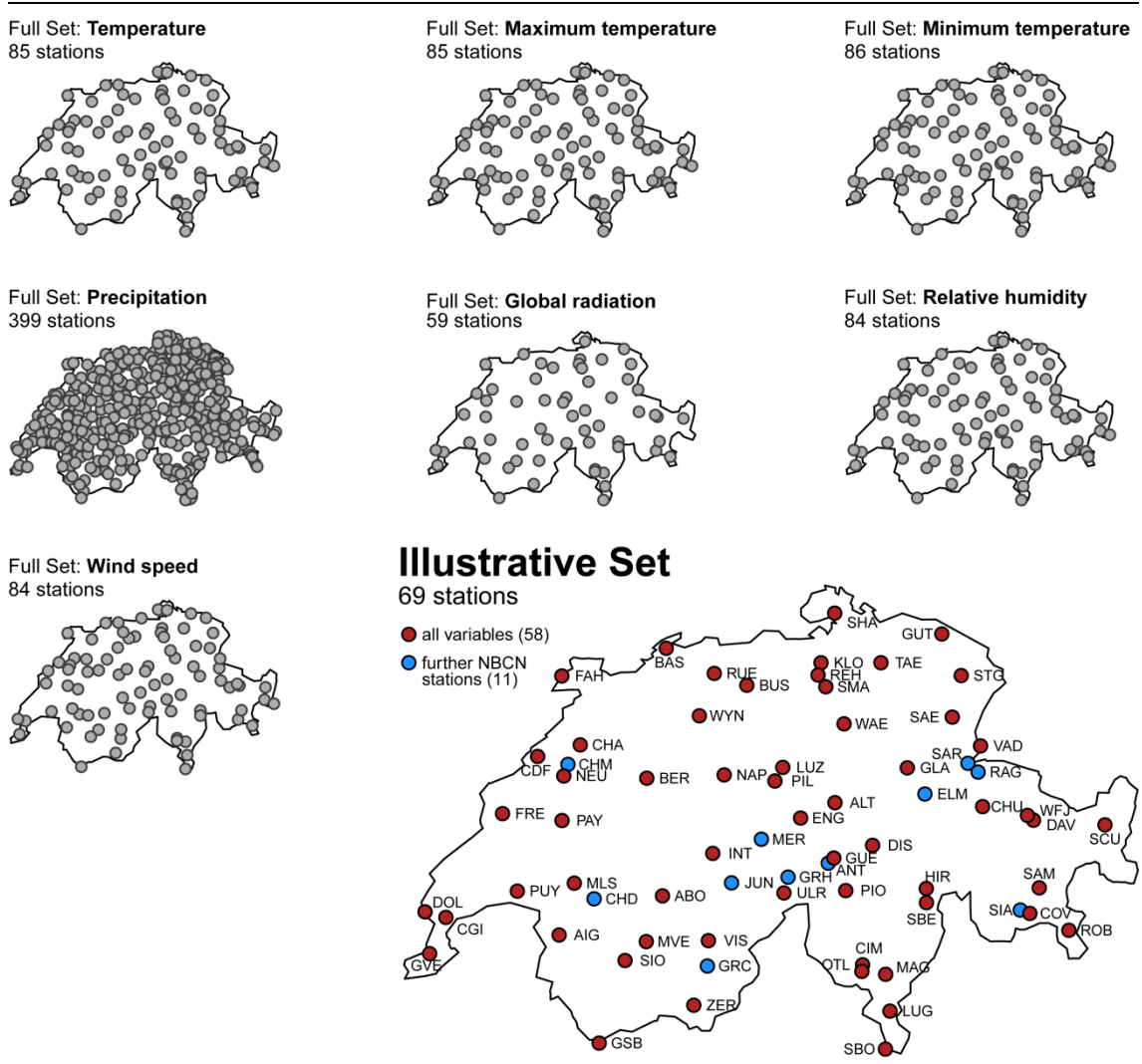


Figure 5: Station sets considered. The small panels denote the full station set for which transient scenarios are provided. The number of available stations depends on the specific variable considered. The lower right panel shows the illustrative set used to illustrate the basic results in both the present report and in the CH2018 Technical Report.

2.5 QM on RCM grid (Setup B)

The QM on the RCM grid (Setup B) does not include a downscaling component since the model data are mapped onto an observation-based grid with the same resolution as the RCM. Setup B represents a mere climate model bias correction and is not provided to end users by default. Its primary

purpose is to assess uncertainties of climate change signals at larger spatial scales (CH2018 regional domains) and to evaluate potential modifications of the raw climate change signal by QM.

Several gridded observational datasets have been merged to provide the reference observations for this QM setup. As a large-scale background data reference, the gridded E-OBS dataset (Haylock et al. 2008) which is available for the whole EURO-CORDEX domain at 25 km resolution is employed. For constructing a reference on the higher-resolved EUR-11 grid, E-OBS has been spatially remapped (nearest neighbor remapping) from 25 to 12 km. Over the Alps the E-OBS reference is replaced by spatially aggregated high-resolution gridded observations (first-order conservative remapping): Over Switzerland the 2 km gridded datasets of MeteoSwiss (TabsD, TminD, TmaxD, RhiresD) are used; in addition, for precipitation outside of Switzerland the Alpine Precipitation Grid Dataset (APGD) with 5 km resolution (Isotta, et al., 2014) is employed. For obtaining an observational reference at the coarser EUR-44 resolution, the merged EUR-11 reference grid was spatially aggregated (first-order conservative remapping) from 12 to 50 km resolution.

2.6 QM to high-resolution grid (Setup C)

QM to high-resolution grid (Setup C) again includes a downscaling step in addition to a bias correction. In contrast to Setup A, QM is applied in a spatially explicit manner yielding complete spatial grids of downscaled and bias-corrected data which are provided to users on request. Prior to QM the model data were conservatively remapped from the original RCM grid (EUR-11 or EUR-44) to the 2 km grid of the observational reference using the CDO operator *cdo remapcon*. As observational reference the MeteoSwiss 2 km gridded products TabsD, TminD, TmaxD (MeteoSwiss 2016a) and RhiresD (MeteoSwiss 2016b) were used. Since these data are only available for the area of Switzerland, the resulting QM product covers Switzerland only. Note that the spatially continuous application of QM with a downscaling component is associated with certain caveats (see below and the CH2018 Technical Report), and the 2 km gridded QM product has to be used with special care.

2.7 Multi-model combination and pattern scaling

All QM setups (A, B and C) are carried out for the entire CH2018 freeze 2.0 ensemble. For the CH2018 ensemble analysis and visualization, the set of available RCM experiments of the model freeze 2.0 is afterwards recombined into a *multi-model combination*. This procedure is applied for the raw experiments and also for the quantile-mapped data (all setups).

First, EUR-44 experiments for which also a EUR-11 version is available (i.e., an experiment carried out by the same model chain but at higher resolution) are excluded in order to minimize interdependencies. Secondly, in order to provide climate change information for all emission scenarios, a temporal, time slice-based pattern scaling is employed to substitute missing experiments for RCP2.6 or RCP4.5 for which a corresponding experiment for RCP4.5 or RCP8.5 is available. This method is based on changes in the global mean temperature (GMT) as simulated by the driving GCMs (Herger, et al., 2015). For a given scenario period these changes are typically largest in high emission scenarios (e.g., RCP8.5) and the corresponding GMT change for a low emission scenario (e.g., RCP2.6) is reached in an earlier period. This 30-year period (corresponding to the GMT change in a low emission scenario) is searched for in the GCM simulation based on the high emission scenario. The cor-

responding period in the EURO-CORDEX GCM-RCM chain is used as a substitute in case that no GCM-RCM experiment is available for the low emission scenario. For missing RCP2.6 experiments the neighboring scenario RCP4.5 is used if available. If RCP4.5 does not exist, both the RCP2.6 and RCP4.5 scenario are substituted by pattern-scaling the RCP8.5 run. See the CH2018 Technical Report for further details. As a result, the number of (real or substituted) simulations is identical for all RCPs and, depending on the variable, amounts to 15 to 26 (26 simulations for temperature and precipitation and less for further auxiliary variables).

For a given RCP, the overall rule for choosing/excluding and substituting simulations in the multi-model combination can be summarized as

EUR-11 simulations > EUR-44 simulations > EUR-11 pattern scaling > EUR-44 pattern scaling

This means that, first, original simulations are preferred over the pattern-scaled substitution. Second, the higher (EUR-11) resolution is preferred over the lower (EUR-44) resolution.

For derivation of climate change signals in the multi-model combination, three distinct scenario periods are related to the reference period 1981-2010: 2020-2049, 2045-2074 and 2070-2099. For reasons of simplicity, these periods are denoted by the corresponding central year of the time window (2035, 2060 and 2085, respectively).

2.8 Calculation of temperature indices

In contrast to raw RCM data, which are typically subject to systematic biases, the quantile-mapped data can be used to derive simple threshold-based temperature indices. A number of such standard indices are considered in CH2018 in addition to more complex ones. **Table 2** lists those threshold indices that are computed based on the CH2018 QM data and their respective definitions.

Table 2: Temperature threshold indices calculated from quantile-mapped data.

Index name	Criterion
Hot days	$T_{\max} > 30 \text{ }^{\circ}\text{C}$
Summer days	$T_{\max} > 25 \text{ }^{\circ}\text{C}$
Tropical nights	$T_{\min} > 20 \text{ }^{\circ}\text{C}$
Frost days	$T_{\min} < 0 \text{ }^{\circ}\text{C}$
Ice days	$T_{\max} < 0 \text{ }^{\circ}\text{C}$

3 Results

In the following we present exemplary and summary results of the QM application in the context of CH2018. First, we verify and evaluate the QM implementation. For this purpose the full calibration period 1981-2010 (or 1981-2008 for Setup B) is considered. This means that evaluation and validation period are identical and no independent cross-validation exercise is carried out. The latter was covered by previous works (e.g. (Ivanov and Kotlarski 2017, Gutiérrez et al. 2018) which revealed that QM, in general, performs well in a historical cross-validation setting with independent calibration and validation periods. In the present report, we focus on a more technical evaluation of the QM implementation based on a comparison of the quantile-mapped data and observations within the calibration period itself in order to identify potential errors or shortcomings of the implementation. For the evaluation exercise we here mostly focus on one individual exemplary model simulation¹, but also consider ensemble median statistics in some cases. Second, we present exemplary results of the QM-based climate scenarios focusing on QM to stations (Setup A).

3.1 QM evaluation: Individual models

QM is massively applied in the context of CH2018. A large number of climate model simulations (each one spanning 119 simulation years from 1981–2099), several hundred stations and/or grid cells and up to seven meteorological parameters are considered (see above). The output produced has a size of several terabytes. Although the general performance of QM has been verified in previous works, problems in individual cases cannot be ruled out. Therefore, a number of control sheets and control figures have been designed which are automatically produced for each QM application (i.e., for each quantile-mapped climate model chain, each variable and, for the case of QM setup A, for each station considered). Below we present examples of this control output, focusing on one exemplary model simulation only (CLMCOM-CCLM4-MPIESM-EUR11-RCP85).

3.1.1 QM to stations (Setup A)

Figure 6 shows an example for a control sheet of QM setup A (QM to stations) for the case of temperature. The upper panels compare annual cycles and seasonal² PDFs of observational data, RCM raw data and quantile-mapped model data. The four lower panels provide details on the QM correction function (averaging the quantile-based correction function over all DOYs within a given season)

¹ CLMCOM-CCLM4-MPIESM-EUR11-RCP85, denoting the RCM *CLMcom-CCLM4-8-17* driven by the GCM *MPI-M-MPI-ESM-LR* at *EUR-11* resolution and for emission scenario *RCP8.5*

² DJF: Winter (December–February), MAM: Spring (March–May), JJA: Summer (June–July), SON: Autumn (September–November)

and on the frequency at which different parts of the function (i.e., quantiles with respect to the control period 1981–2010) are used in the future scenario period (here 2070–2099).

In the specific case shown, the raw RCM approximately captures mean winter, spring and autumn temperatures in the reference period 1981–2010, although the distribution of daily data is too narrow in most cases. Summer temperatures are underestimated by approx. 2°C, again, with a too narrow distribution of daily values compared to observations. QM corrects for these biases (compare the red and the black lines and numbers). Furthermore, the quantile-mapped data reproduce the main features of the mean annual cycle of the temperature change as represented by the raw RCM data (central right hand panel). Especially in wintertime, however, QM tends to increase the raw model's temperature change signal by several tens of a degree. Such a modification of the change signal by QM can be meaningful in case of intensity-dependent model biases but could also point to statistical artifacts (see Chapter 4). The quantile-based mean seasonal correction functions (lower panels) mostly reveal a positive slope, implying a stronger upward correction of simulated temperatures for high quantiles than for low quantiles. This feature of the correction function directly results from the fact that the simulated distributions are mostly too narrow (see above); a positively sloped correction function generally increases the distributional width of the raw PDF. Also note that temperatures in the scenario period more often reflect high calibration period quantiles than low quantiles (dashed gray lines in the four lower panels), especially in summer. In combination, this implies that the mean upward QM correction in the future scenario period is stronger (or the mean downward correction weaker) compared to the historical reference period, leading to a somewhat larger climate change signal in the quantile-mapped data compared to the raw RCM (see above and Chapter 4).

The corresponding exemplary control sheet for precipitation is shown in **Figure 7**. The raw RCM considerably overestimates observed precipitation during the entire year. The same is true for the wet day frequency. Again, QM corrects for these biases and also represents the basic characteristics of the raw model's change signal (increase of precipitation in winter, spring and autumn; decrease in summer) with a certain modification especially in wintertime. As the PDFs are based on all days (dry and wet) lower quantiles represent dry days (below 0.1 mm/day). The correction function amounts to zero for these lower quantiles. Between the 30th and the 40th quantile, the correction function starts to become negative. It is in this quantile range, where the correction turns wet days of the raw model into dry days and hence leads to a correction of the wet-day frequency. For medium to high quantiles the correction is mostly negative, implying a downward correction of simulated precipitation in order to match observational quantiles.

In principle, the results for the exemplary model chain and the exemplary station shown also apply to all other cases. QM is able to appropriately correct distributional model biases in the reference period in all cases. The shape and location of the correction function, however, can differ from case to case. For temperature, the mean model biases mainly reflect elevation differences between the station considered and the respective climate model grid cell and, hence, the scale gap between climate model and observations. As such, it strongly depends on the station considered. Furthermore, depending on the station and climate model chain, the modification of the climate change signal by QM can be slightly more or slightly less pronounced compared to the example shown here.

CH2018 QM station control: **Daily temperature (tas)**

SMA CLMCOM-CCLM4-MPIESM-EUR11-RCP85

Calibration period: 1981–2010, Scenario period: 2070–2099, QM version: v08

— CAL/CTRL — Obs
 - - - SCEN — RCM raw
 — QM

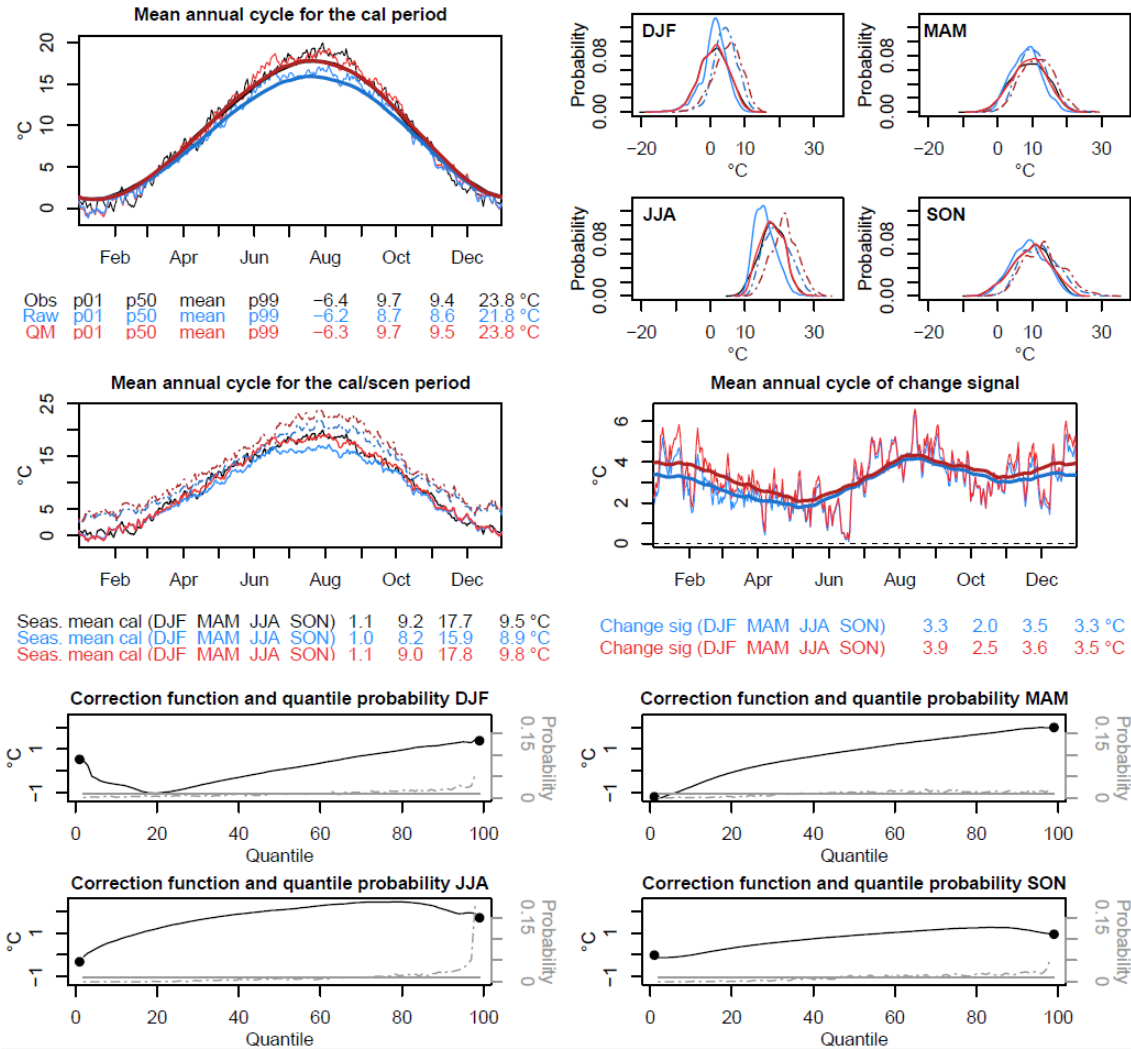


Figure 6: QM to stations control plot for Zurich/Fluntern (SMA), model chain CLMCOM-CCLM4-MPIESM-EUR11-RCP85 and temperature (tas). Mean annual cycles and PDFs are shown for the observations (black), raw model data (blue) and quantile-mapped data (red). Numbers indicate seasonal mean values (p01: 1st percentile, p50: 50th percentile, mean: mean, p99: 99th percentile, Seas. mean cal.: seasonal mean value in the calibration period, Change sig: seasonal mean climate change signal). In the four lower panels the mean seasonal correction function (left y-axis) and the seasonal PDFs of the scenario values mapped into the quantile probabilities of the calibration period (right y-axis) are shown. The horizontal gray line denotes the probability of the calibration period quantiles (0.01 for 100 percentiles, by definition).

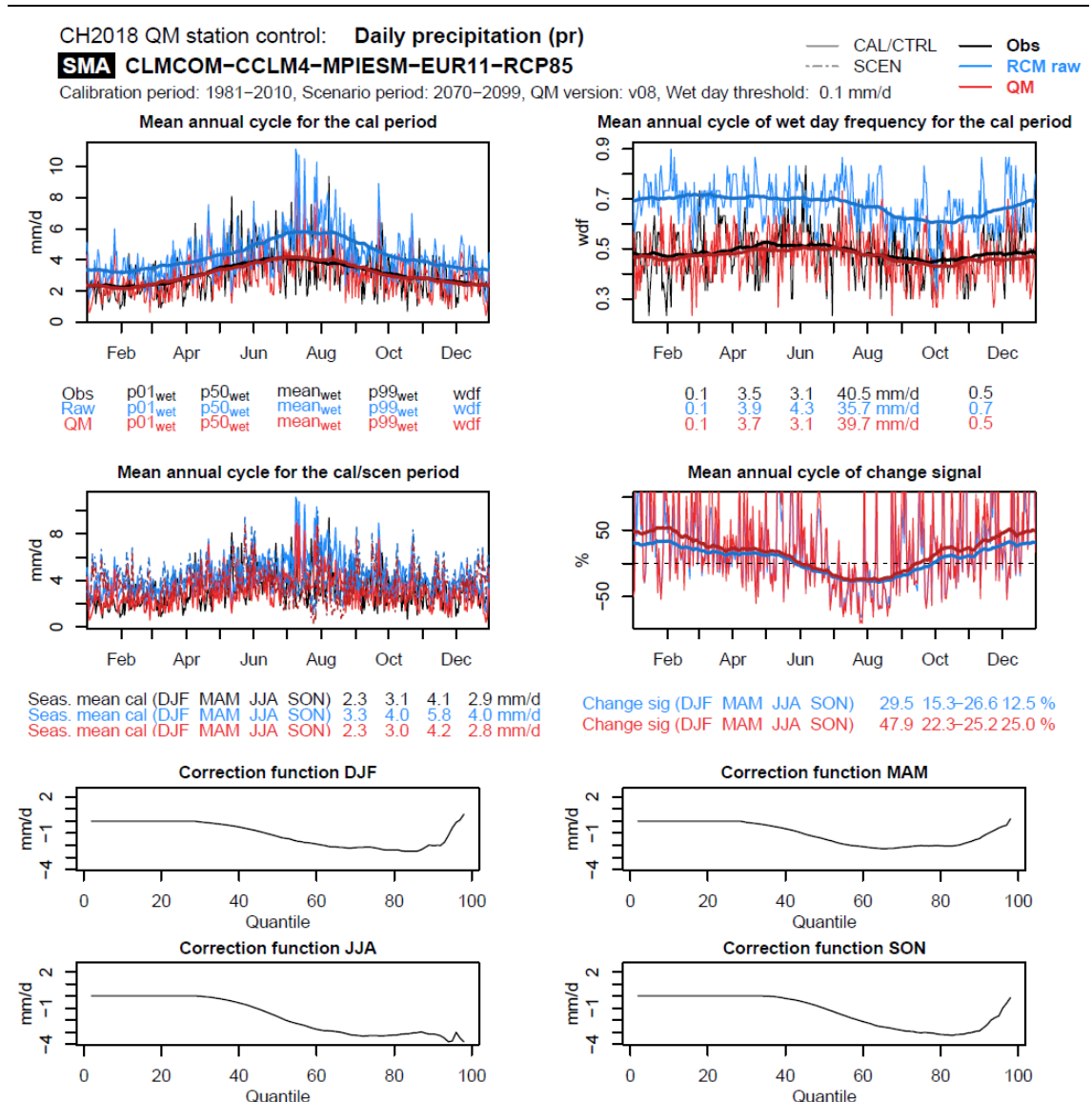


Figure 7: As **Figure 6** but for precipitation and with two adjustments: The upper right panel shows the mean annual cycle of the wet day frequency in the respective datasets instead of the four seasonal distributions. PDFs of the scenario period values are omitted in the four lower panels.

3.1.2 QM on RCM grid (Setup B)

In the case of QM on the RCM grid (Setup B), the bias correction has been carried out independently for each RCM grid cell in the domain. Producing the same control sheets as for Setup A for each grid cell would result in an unmanageable number of figures. Hence, only summary evaluations in terms of spatial patterns of seasonal mean values in the observations, in RCM raw output and in quantile-mapped output are produced operationally. For individual cases, however, detailed evaluations as shown in **Figure 6** and **Figure 7** can be produced.

An exemplary evaluation sheet for QM on the RCM grid and for the case of temperature is shown in **Figure 8**. The upper part presents the pattern of seasonal mean temperatures in the three datasets

in the calibration period 1981–2008, the lower part the seasonal mean biases of RCM raw and of quantile-mapped output when compared against the observational reference. The specific RCM considered here is subject to a pronounced and widespread cold bias of partly more than 2°C, except for the Swiss midlands in winter. After application of QM these biases of seasonal means almost vanish and are reduced to a few tens of a degree at maximum. Such remaining biases in the calibration period can be explained by the approximate nature of the QM implementation (use of the 99 empirical percentiles with linear interpolation in-between) which avoids overfitting and by the use of a 91-day moving window for calibration. The latter implies the consideration of days outside the evaluated 3-month season (e.g., considering days in January and March for correcting February days). Hence, the QM product can only approximate the fixed-period seasonal mean values (see **Figure 3**).

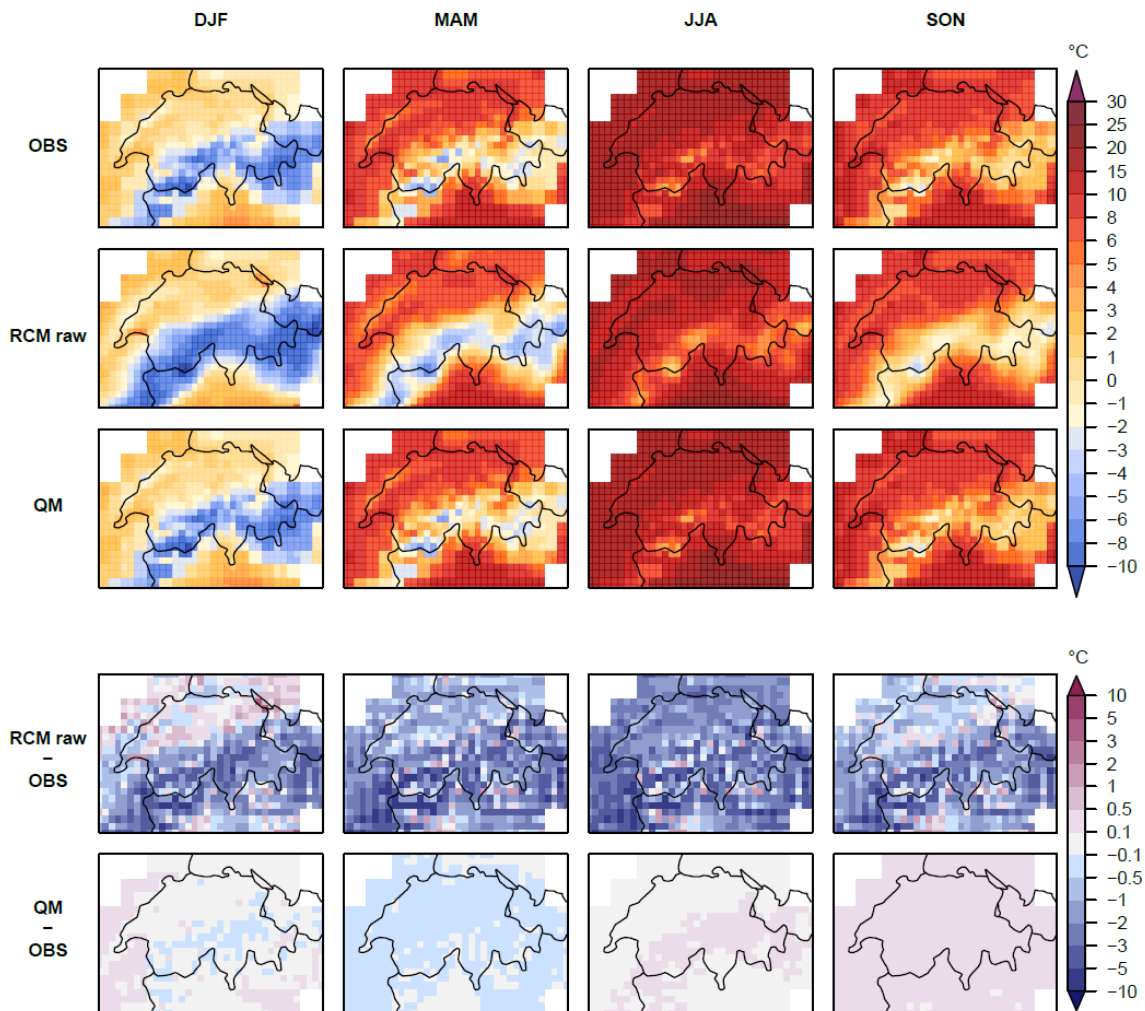


Figure 8: QM on RCM grid control plot for the model chain CLMCOM-CCLM4-MPIESM-EUR11-RCP85 and temperature (tas). The upper rows show the spatial distribution of seasonal mean temperature in the QM calibration period 1981-2008 for the reference observations (OBS), the raw RCM data (RCM raw) and the quantile-mapped data (QM). The two lower rows show the spatial pattern of the seasonal mean bias of raw and of quantile-mapped RCM data.

For the case of seasonal mean precipitation (**Figure 9**) the RCM is subject to a pronounced wet bias in almost the entire model domain. Note that part of this bias could arise from the fact that the observational reference has not been corrected for the systematic undercatch of precipitation gauges (e.g. Sevruk 1997). Again, QM effectively corrects for the model bias, and the quantile-mapped data are subject to minor remaining seasonal mean biases.

The effective correction of raw model biases by QM in the calibration period does not only apply to the exemplary model experiment CLMCOM-CCLM4-MPIESM-EUR11-RCP85 but is valid for all other experiments as well.

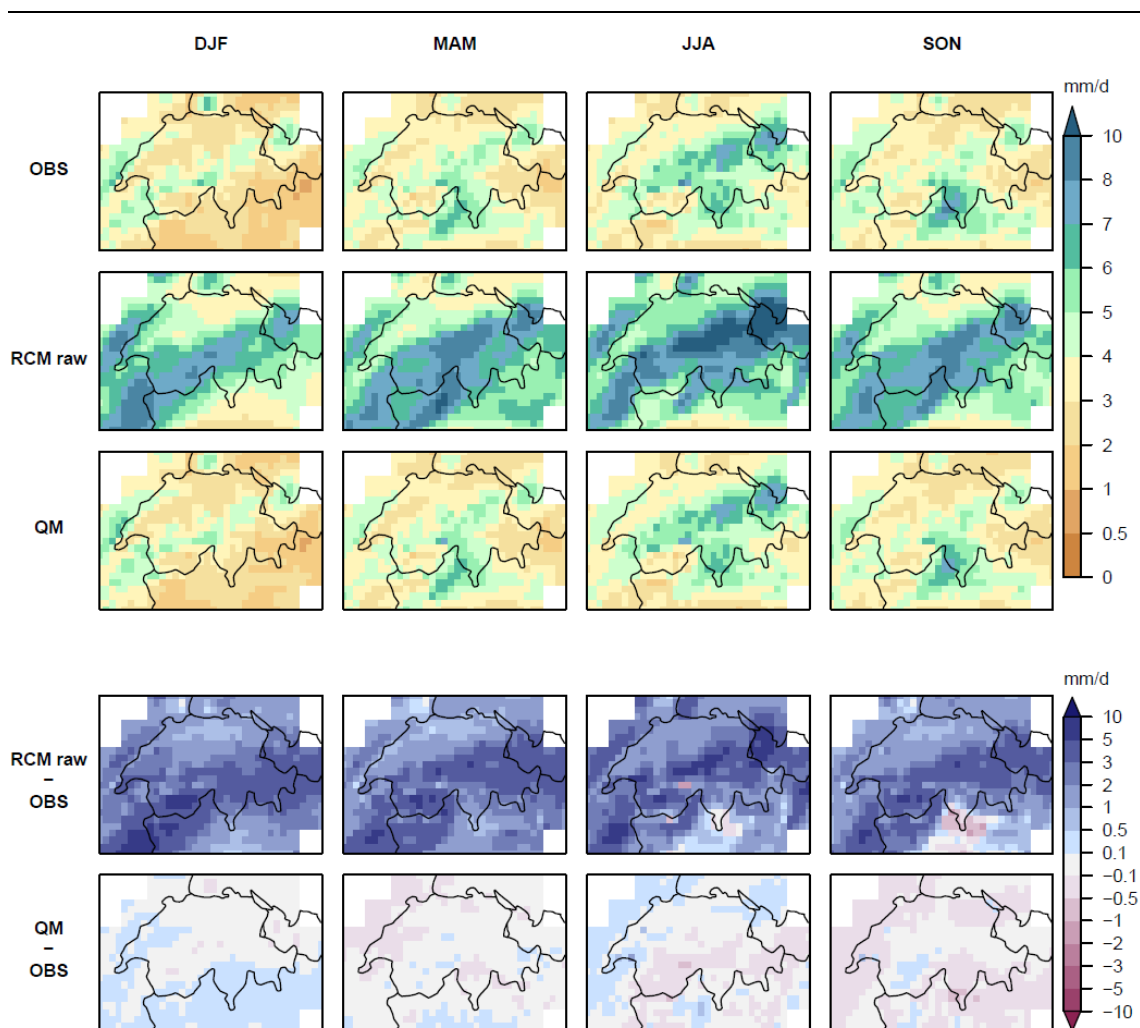


Figure 9: As **Figure 8** but for precipitation.

3.1.3 QM to high-resolution grid (Setup C)

Similar to Setup B, an operational evaluation of QM to the high-resolution grid (Setup C) is not carried out for each individual quantile-mapped grid cell but in a summarizing manner only. **Figure 10** shows an exemplary evaluation sheet for temperature. The components of this sheet are identical to those presented above for Setup B, but evaluation is now carried out at the higher 2 km resolution.

As explained in Chapter 2.6, raw model data were conservatively remapped to this higher spatial resolution before the application of QM. The corresponding spatial variability of seasonal mean temperature is therefore much lower in the raw RCM output compared to the observational 2 km reference (compare first and second line in **Figure 10**). The spatial pattern of the mean biases of RCM raw (fourth row) is mainly governed by topographic features, reflecting the elevation difference between the topography of the 2 km grid-resolution of the observational reference and the strongly smoothed original RCM topography. The predominant bias pattern is characterized by cold biases in the valleys (RCM grid cell at a higher elevation than 2 km grid cells, implying a systematically lower temperature) and warm biases aloft (RCM grid cell at a lower elevation, implying a systematically higher temperature). As expected, QM effectively corrects for these biases and produces spatial temperature patterns that closely resemble those of the observations. Remaining biases are small and still subject to a slight topographic control (bottom row in **Figure 10**).

Also for precipitation, spatial variability in the interpolated raw RCM data is much smaller than in the observational reference (**Figure 11**). As already apparent from Setup B (see Chapter 3.1.2), the specific RCM under consideration suffers from a pronounced wet bias in all seasons and over most parts of the analysis domain. Due to a less pronounced dependence of seasonal precipitation means on elevation, the spatial bias pattern of raw RCM output is less controlled by topography than in the case of temperature (fourth row in **Figure 11**). QM effectively removes the bias of the raw data, and the resulting quantile-mapped product only shows minor remaining biases (bottom row).

Again, the results presented for the exemplary model experiment CLMCOM-CCLM4-MPIESM-EUR11-RCP85 with respect to the ability of QM to correct for raw RCM biases in the calibration period also apply for all other experiments considered in this work.

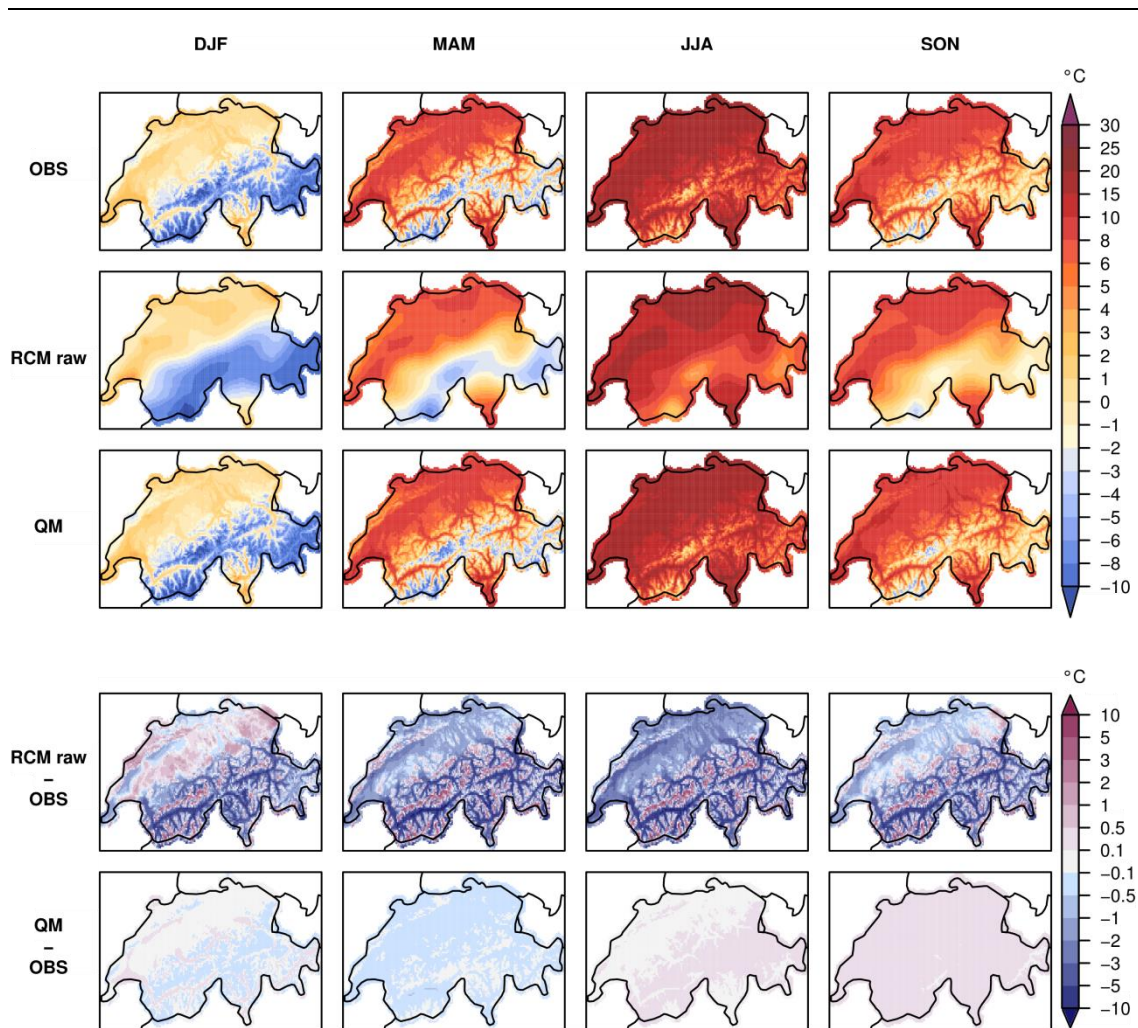


Figure 10: Control plot for QM to the high-resolution grid for the model chain CLMCOM-CCLM4-MPIESM-EUR11-RCP85 and temperature (tas). The upper rows show the spatial distribution of seasonal mean temperature in the QM calibration period 1981-2008 for the reference observations (OBS), the interpolated raw RCM data (RCM raw) and the quantile-mapped data (QM). The two lower rows show the spatial pattern of the seasonal mean bias of raw and of quantile-mapped RCM data.

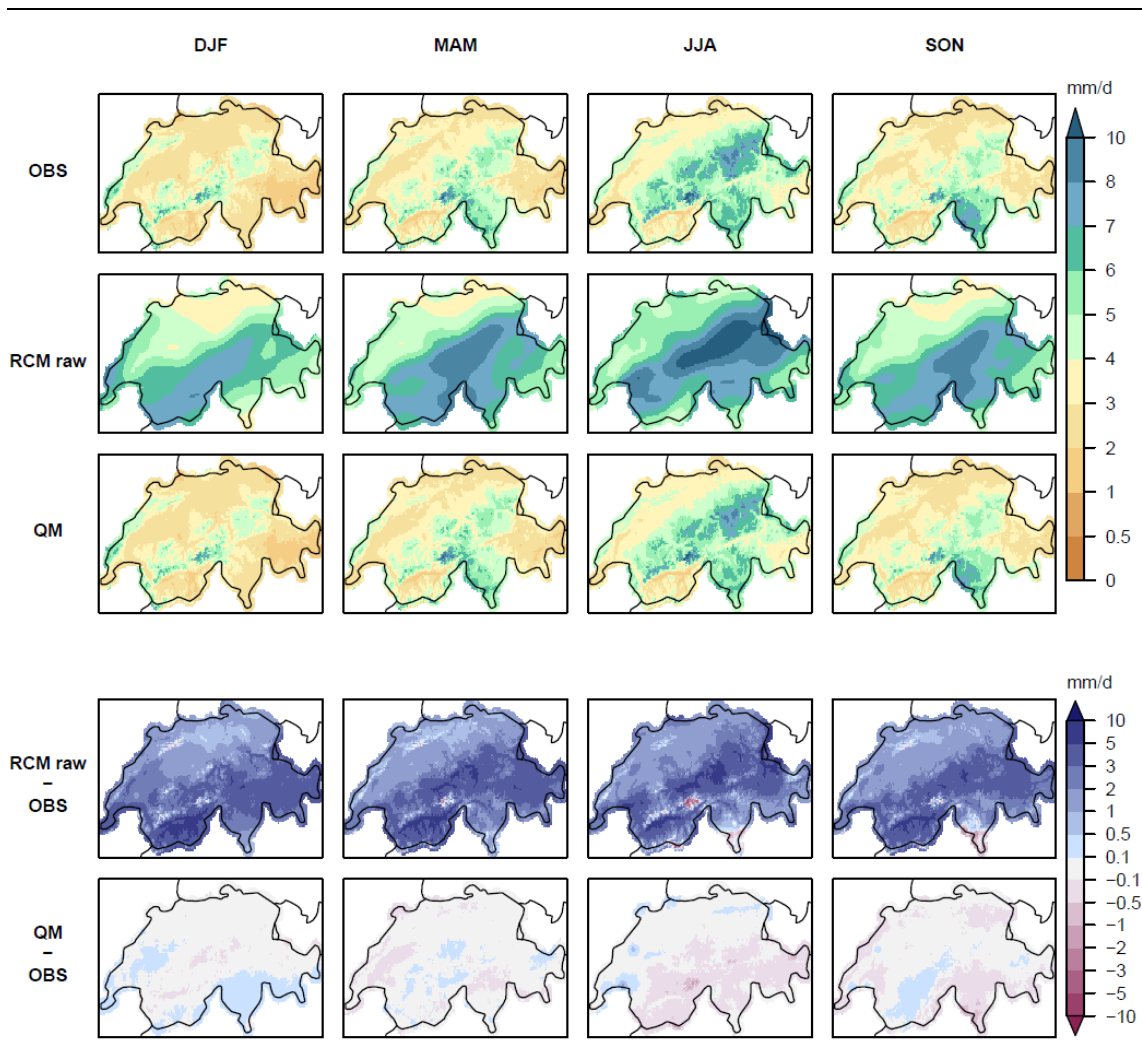


Figure 11: As Figure 10 but for precipitation.

3.2 QM evaluation: Model ensemble

In addition to evaluation sheets for all individual QM applications (Setup A) or summary evaluation sheets for all individual RCM experiments (Setups B and C) as presented above, additional standard evaluations are performed for the ensemble median of all quantile-mapped RCM experiments considered. These evaluations provide an overview on the biases of the entire RCM ensemble and the ability of QM to correct for these biases in the calibration period. They are carried out for QM Setups A, B and C. Here, we provide examples for Setup A (QM to stations) and for the variables temperature, precipitation and global radiation only. Results in terms of bias removal by QM are similar for all three setups.

While the general geographical and temporal pattern of seasonal mean temperature is captured well by the RCMs, an underestimation at most sites and in all seasons is apparent (Figure 12). Presumably, this cold bias is mostly related to the scale mismatch inherent to this kind of evaluation and to the fact that most stations are located in valleys and at lower elevations, i.e. in a systematically warmer

environment, than their corresponding overlying RCM grid cell. After application of QM these apparent temperature biases are removed to a large extent. The remaining ensemble median biases mostly range between ± 0.5 °C. A notable systematic feature is a remaining cold bias at most stations in spring. The evaluation of seasonal mean precipitation (**Figure 13**) reveals a wet bias of the raw RCMs at most sites and in all seasons. Again, QM effectively reduces these biases. The remaining differences to the observational reference are small and do not exceed ± 0.5 mm day⁻¹. In summer, a systematic underestimation of observed precipitation by 0.1 to 0.5 mm/day remains. Finally, the evaluation of global radiation (**Figure 14**) indicates an overestimation by the raw models at most sites except for a few locations along the main Alpine ridge. QM reduces these biases to less than ± 5 W m⁻² with a remaining systematic underestimation in wintertime.

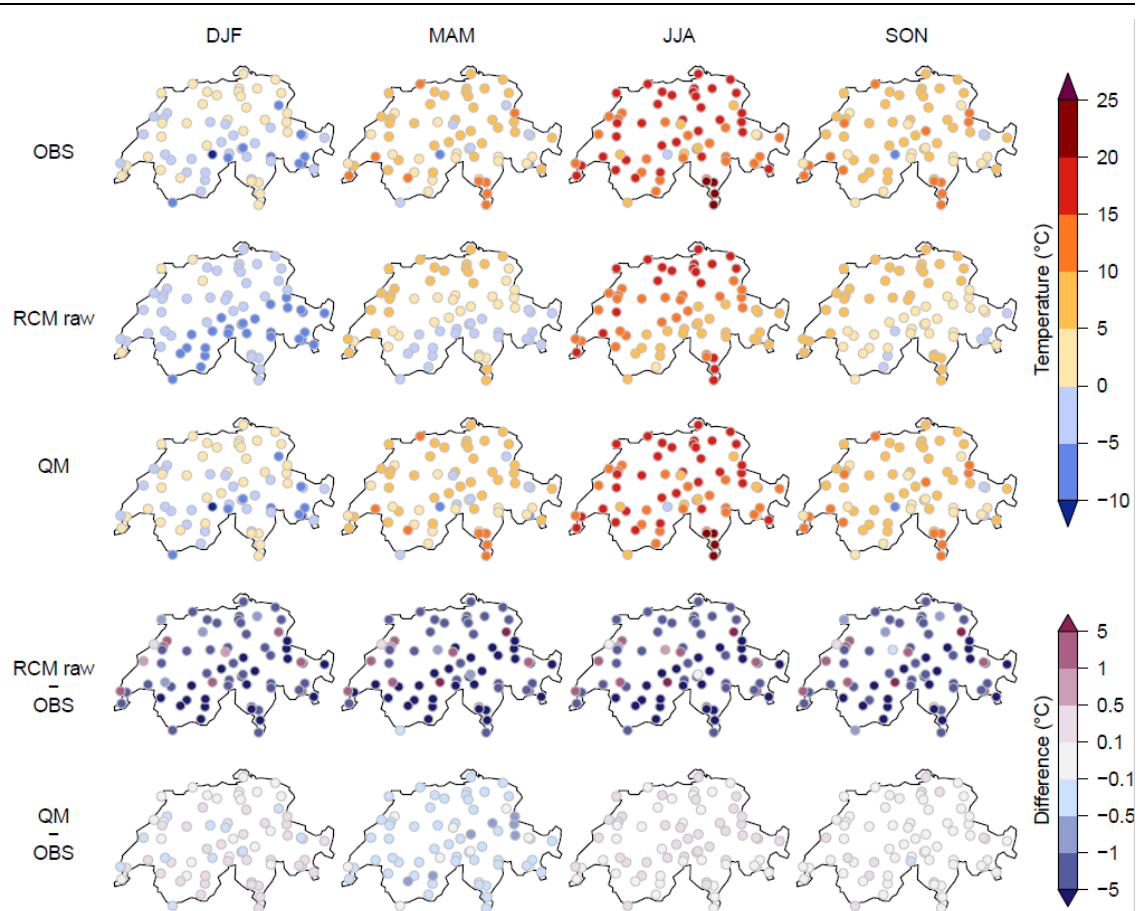


Figure 12: Spatial pattern of seasonal mean temperature in the observations (first row), in RCM raw data (second row) and in the quantile-mapped product (third row). Ensemble median for the calibration period 1981 – 2010 for Setup A (QM to stations). In all cases raw RCM data refers to the simulated series of those RCM grid cells in which the respective station is located.

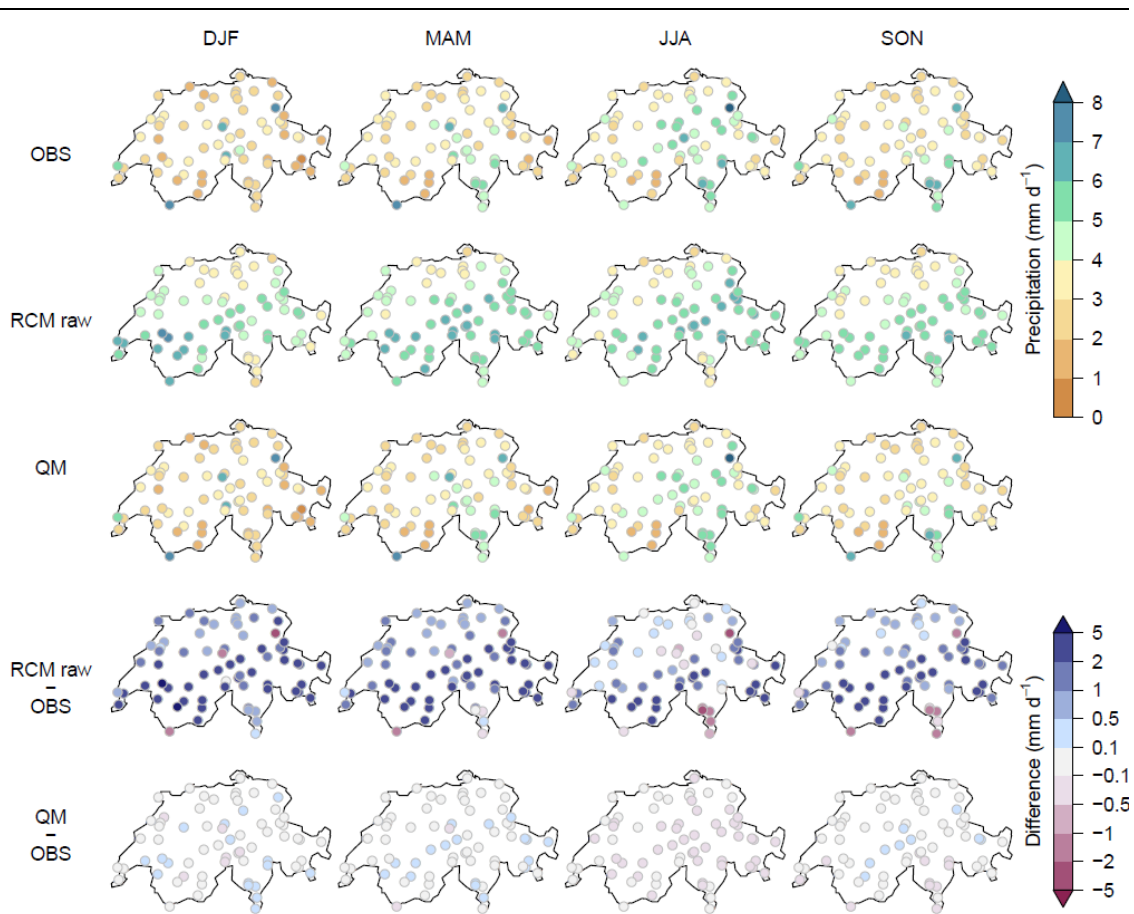


Figure 13: As Figure 12 but for seasonal mean precipitation.

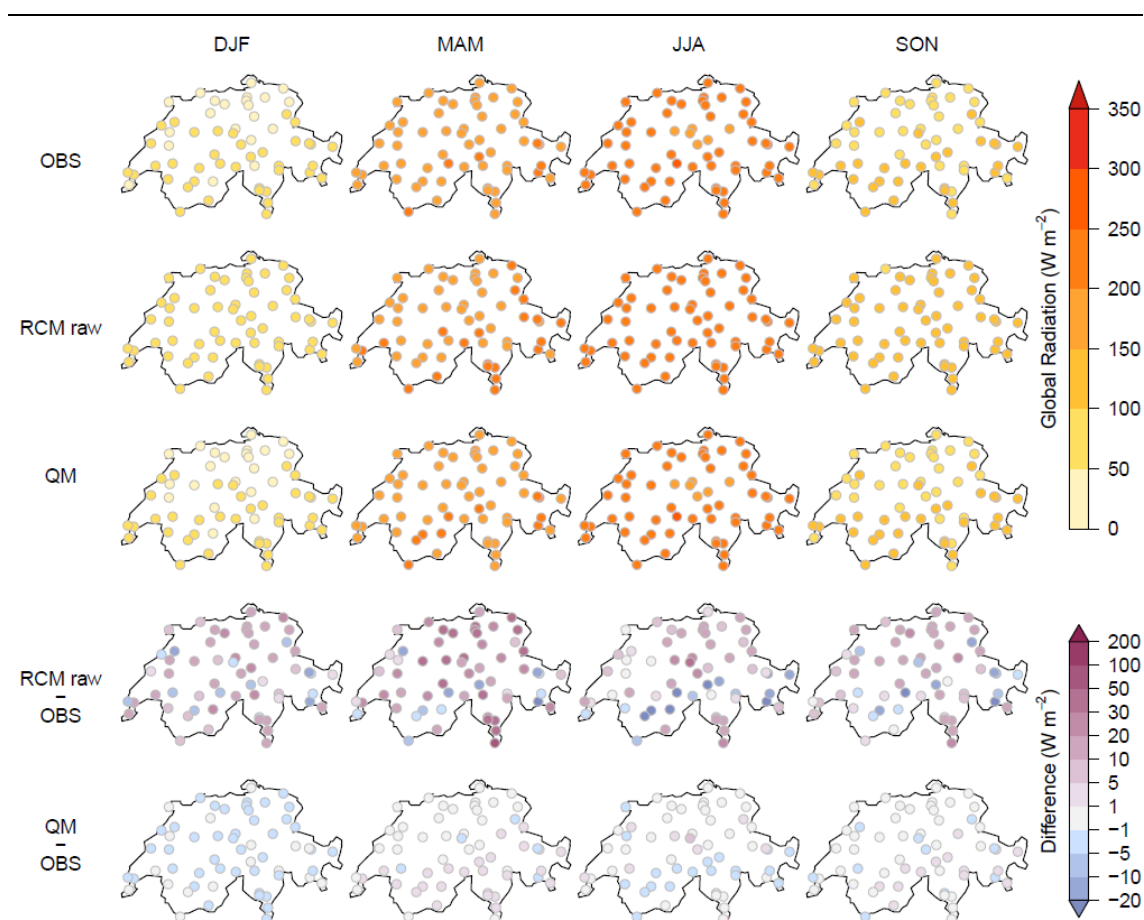


Figure 14: As Figure 12 but for seasonal mean global radiation.

3.3 QM scenarios

In the following, an overview of the climate change signals of several variables and related indices for QM Setup A (QM to stations) is presented. These results are exemplary and are largely consistent with the gridded QM Setups B and C. A more detailed presentation and analysis of the climate change signals can be found in the CH2018 Technical Report.

The spatial pattern of the seasonal mean temperature change for RCP8.5 (Figure 15) is rather homogenous but is slightly amplified over the main Alpine ridge in summer and autumn and by the end of the century (lower row). Here, ensemble median temperature increases of more than 5°C are projected by the end of the century while a warming between 3 and 5°C prevails over most other parts of the country. For the early scenario period 2035, climate change signals do not exceed 2°C (upper row). Figure 16 shows the present-day and the projected future (2085) mean annual cycle of temperature at four exemplary sites and for all three emission scenarios. Climate change won't modify the characteristics of the mean annual cycle but will be associated with temperature increases throughout the entire year. These increases are strongest for RCP8.5 and weakest for RCP2.6. Model uncertainty can be large, in particular for RCPs 4.5 and 8.5. But especially for RCP8.5 even

the lower limit of the uncertainty range is associated with a pronounced temperature increase with respect to present-day conditions at all sites and throughout the entire year.

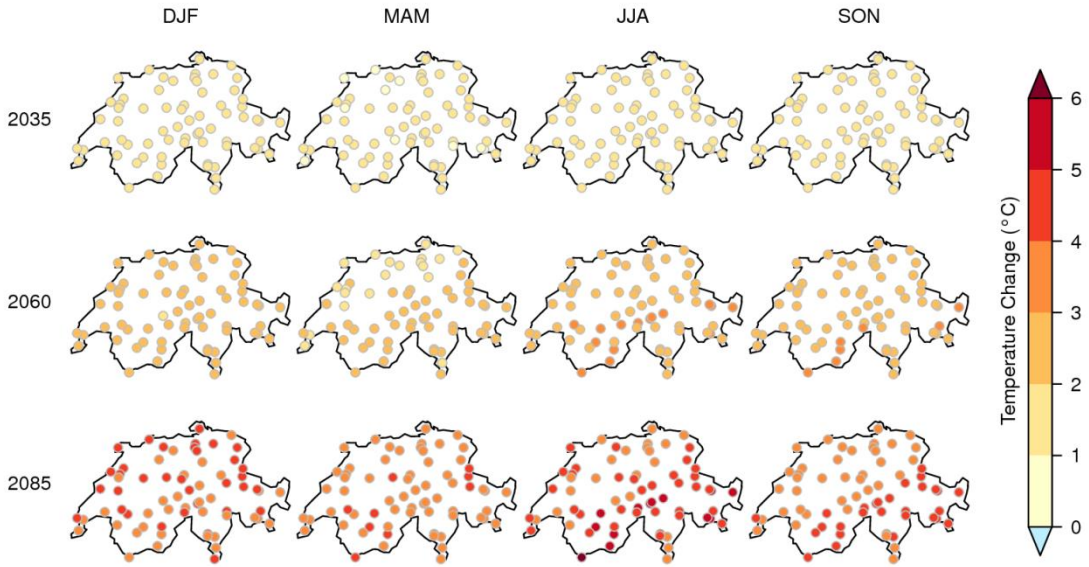


Figure 15: Ensemble median climate change signal of seasonal mean temperature (Setup A, QM to stations) for the three scenario periods and for RCP8.5 (multi-model combination).

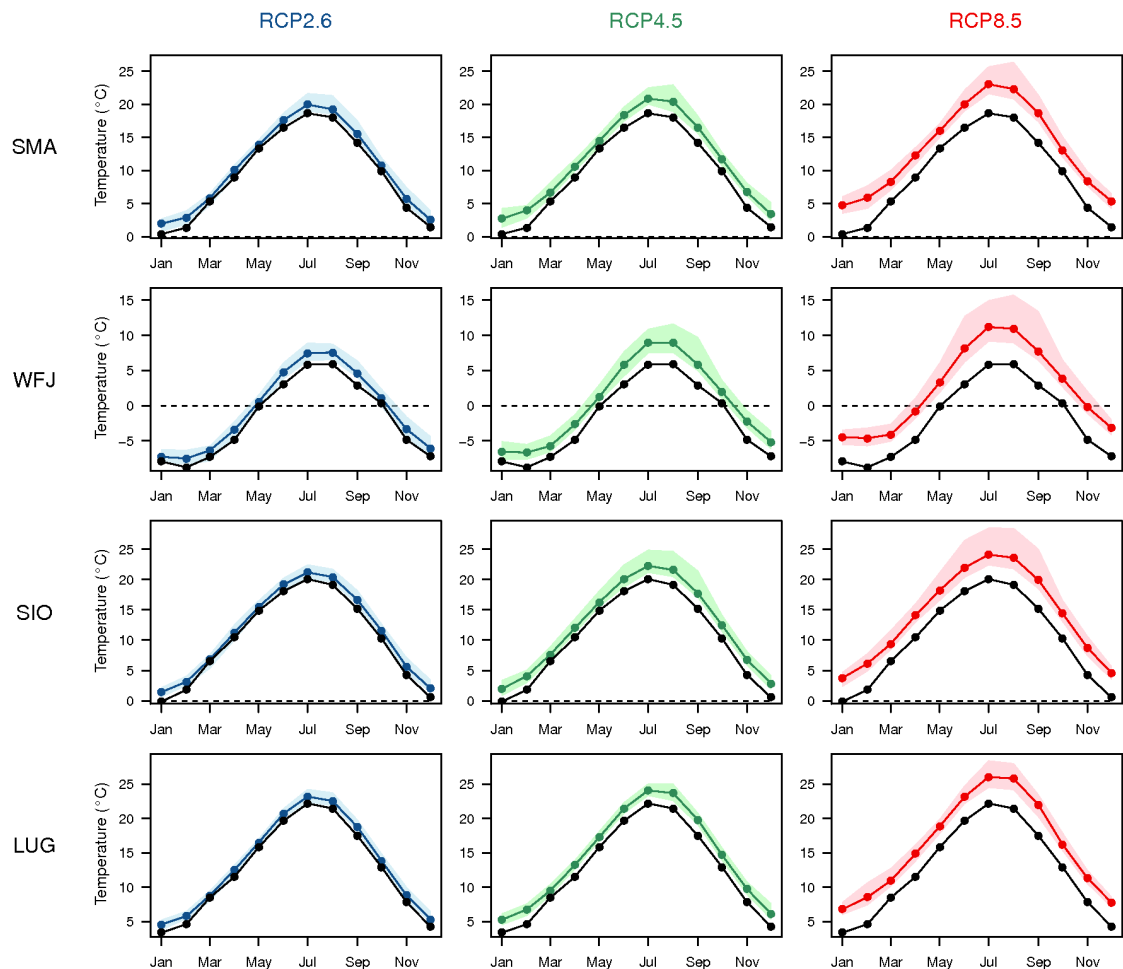


Figure 16: Mean annual cycle of temperature for the reference period (observations, black) and the scenario period 2085 (multi-model combination for Setup A, colored) for all RCPs (columns) and the four exemplary sites of Zurich / Fluntern (SMA), Weissfluhjoch (WFJ), Sion (SIO) and Lugano (LUG). In case of the RCPs the line indicates the ensemble median while the shading indicates the ensemble range.

In contrast to temperature, seasonal mean precipitation changes for RCP8.5 are subject to a pronounced annual cycle that is valid for most parts of the country (**Figure 17**). While precipitation is projected to increase in winter and spring (ensemble median increase typically larger than 10% in winter and 5% in spring), the QM scenarios reveal little change of summer precipitation by 2035 and a pronounced decrease by partly more than 20% by 2085. For autumn, the projected precipitation change is small. The comparison of the present day and the projected future (late scenario period, 2085) annual cycles of precipitation at the four exemplary sites indicates a number of differences (**Figure 18**). At Sion (SIO) the combination of a projected increase of winter and a decrease of summer precipitation could result in a larger magnitude of the secondary winter precipitation maximum and, overall, higher precipitation sums in winter compared to summer. At Lugano (LUG) the secondary September maximum in today's climate might shift to October under all emission scenarios. **Figure 18** also reveals the considerable uncertainty of especially summer precipitation changes. While

ensemble mean changes are predominantly negative in the summer months (decrease of precipitation), individual ensemble members at the upper range can indicate summer precipitation increases.

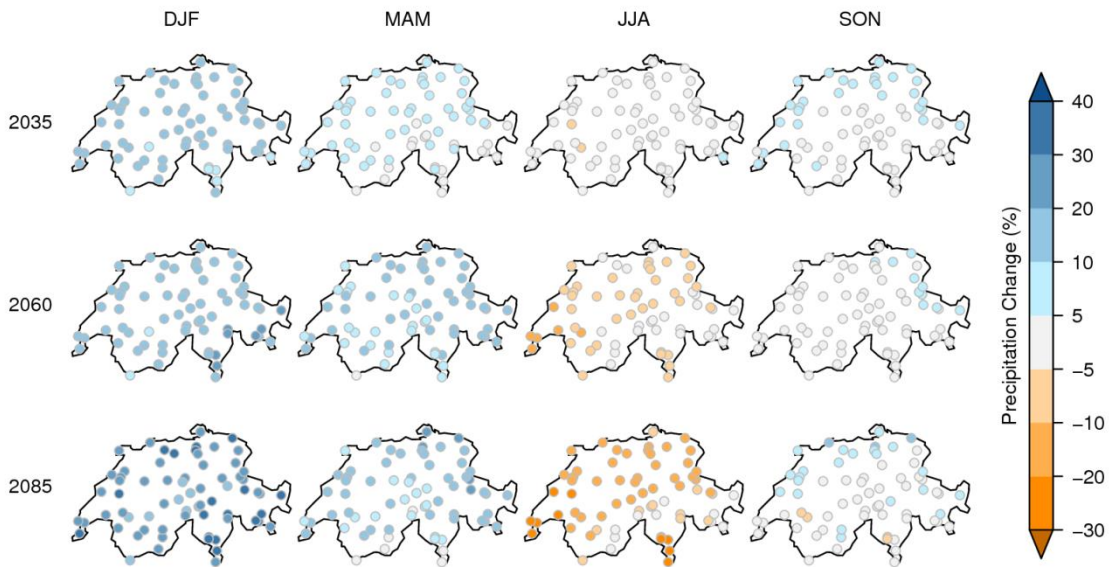


Figure 17: As **Figure 15** but for seasonal mean precipitation. The climate change signal is expressed in relative terms.

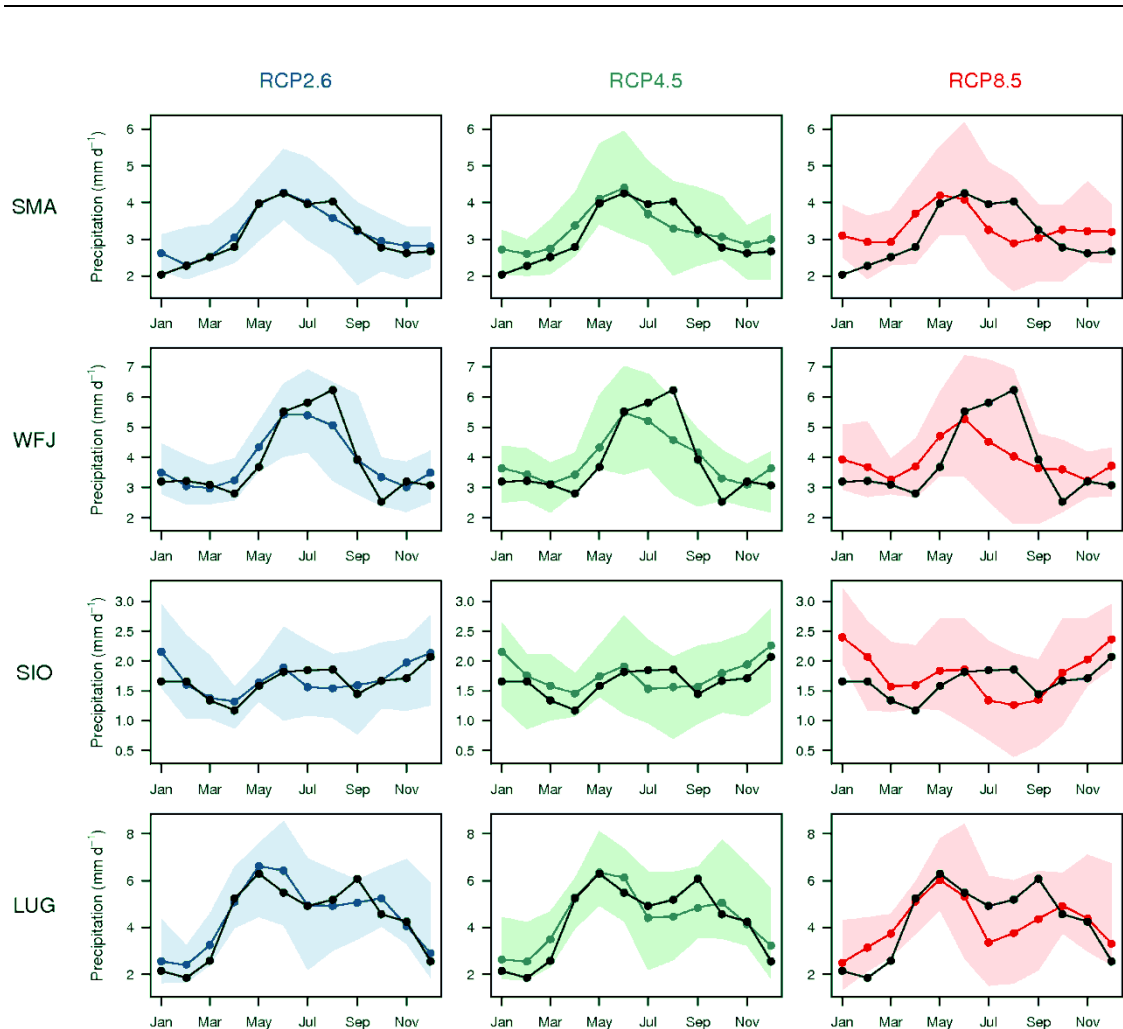


Figure 18: As Figure 16 but for precipitation.

Besides daily mean temperature and precipitation, QM Setup A also considers further meteorological variables (daily minimum and maximum temperature, relative humidity, global radiation and wind speed; cf. **Table 1**). An overview on their projected ensemble median change signals for RCP8.5 and the late scenario period 2085 is provided by **Figure 19**. Seasonal mean changes of daily minimum and maximum temperature (first and second row) show a similar pattern and a similar magnitude as changes of daily mean temperature (see above). Daily maximum temperature changes, however, tend to be slightly more pronounced and, in summer and spring, show a characteristic amplification over the main Alpine ridge. Changes of relative humidity (third row) are small in spring and autumn, while humidity increases up to several percent are apparent in wintertime over the Alps. In summer, a decrease of relative humidity by several percent is projected for most parts of the country (in agreement with, e.g., Sherwood et al. 2010 and Ruosteenoja et al. 2013 for Central Europe). Projected ensemble median changes of global radiation (fourth row) are negative in winter and spring and mostly positive in summer, especially north and south of the main Alpine ridge. Autumn shows little changes. This temporal pattern is strongly connected to the projected precipitation changes (see above) and cloud cover changes are likely to play a dominant role (not analyzed in detail). Finally,

wind speed changes (fifth row) are minor in winter and spring. Small ensemble median decreases are projected for summer and autumn.

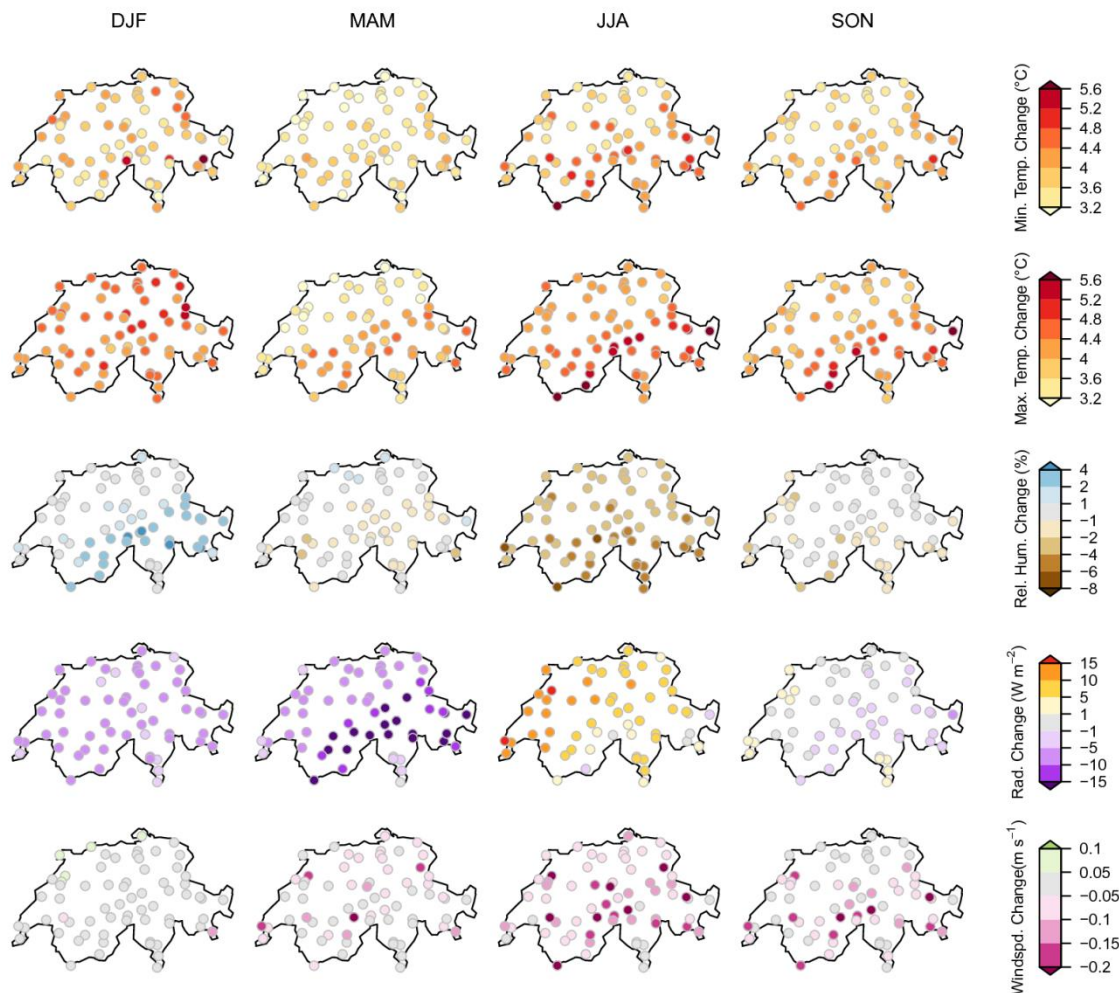


Figure 19: Ensemble median climate change signal (Setup A, QM to stations) of seasonal mean minimum temperature, maximum temperature, relative humidity, global radiation and wind speed (top to bottom) for the scenario period 2085 and for RCP8.5 (multi-model combination).

The projected increase of daily minimum and maximum temperatures as described above will have corresponding effects on the five temperature threshold indices defined in **Table 2**, i.e. on the frequency of hot days, summer days, tropical nights, frost days and ice days. For RCP8.5 their projected evolution for the same four exemplary sites and the three future scenario periods is presented in **Figure 20**. Hot days, summer days and tropical nights are projected to become more frequent in the future. At the Alpine site of Weissfluhjoch (WFJ) the respective temperature thresholds are not reached in the present-day climate but might be surpassed by the mid (summer days) or by the end of the century (hot days, tropical nights). Again, model uncertainty (as represented by the whiskers) can be pronounced, in particular for the late scenario period 2085. Vice versa, the frequency of cold

temperature extremes (frost days, ice days) is projected to decrease throughout the 21st Century. In Lugano (LUG) ice days are already rare in today's climate and might become completely absent by 2085. A frequency decrease of cold temperature extremes is also apparent at Weissfluhjoch.

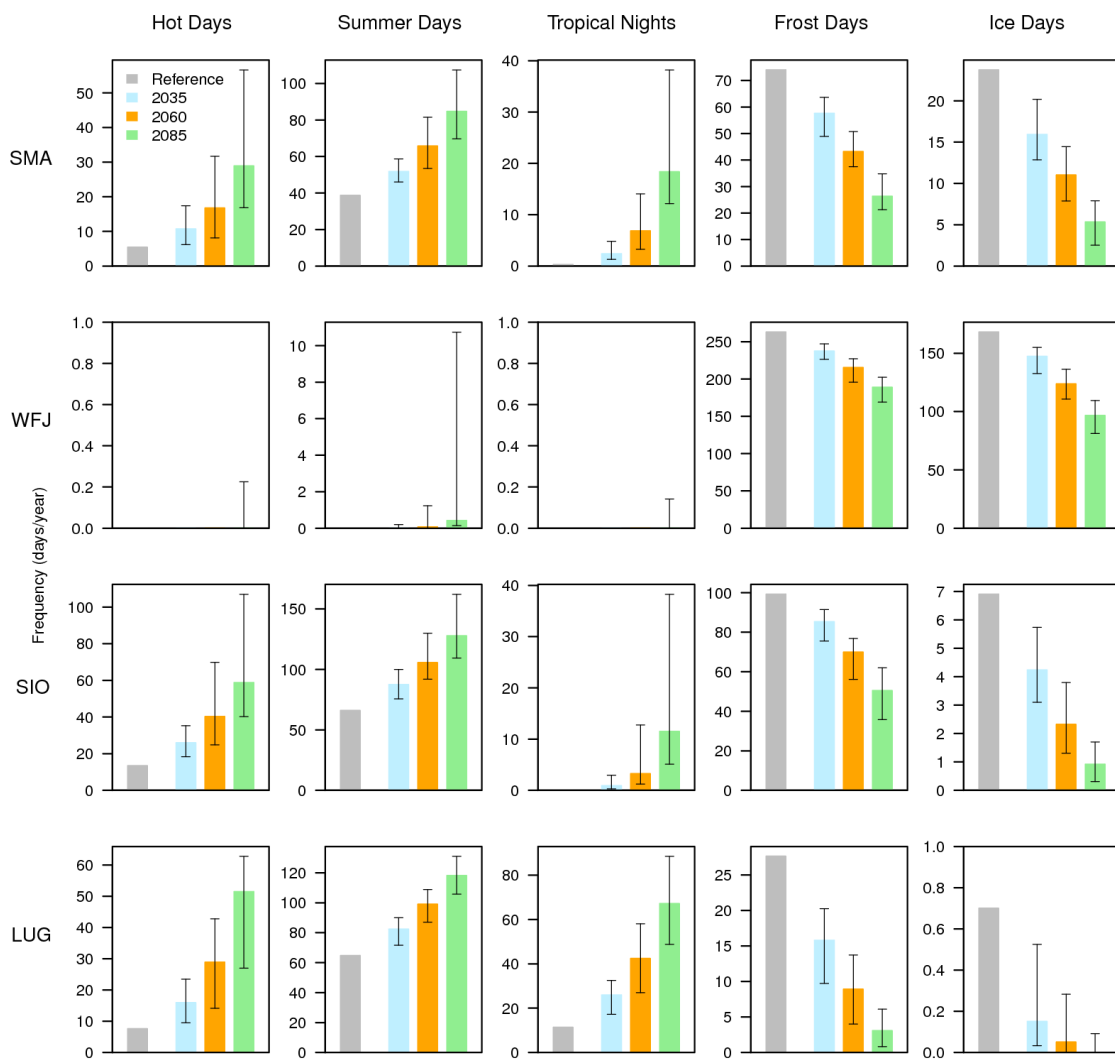


Figure 20: Frequency of hot days, summer days, tropical nights, frost days and ice days in the reference period (observations) and in the three scenario periods (multi-model combination, Setup A) for RCP8.5 and the four exemplary sites Zurich / Fluntern (SMA), Weissfluhjoch (WFJ), Sion (SIO) and Lugano (LUG). The scenario period bars indicate the ensemble median number, whiskers the 5 - 95 % model range.

4 Limitations

Quantile mapping is an attractive and versatile approach for the generation of transient bias-corrected climate scenarios at different spatial scales. It has a number of advantages compared to the delta change method that has been employed for the previous CH2011 scenarios (CH2011 2011). However, QM-based products involve a number of limitations and potential pitfalls. Some of these can speak against the application for specific purposes, and a careful evaluation of the usability of QM-based scenarios is required for any given application. In addition, postprocessing by QM adds another level of uncertainty to the overall uncertainties already inherent to climate model simulations (Wilby and Dessai 2010), in particular for cases where QM is associated with a downscaling step (here: Setups A and C; Maraun, et al. 2017).

In the following, we provide a brief overview on the limitations of the QM-based products that are produced and provided to end users in the context of CH2018. Users should make themselves familiar with these restrictions and to assess the usability of the QM-based CH2018 products for their specific application at hand. Further information can be found in the CH2018 Technical Report and in the referenced literature.

Stationarity of the model bias: QM is calibrated in the historical reference period and is then applied to the entire simulated time series including the future scenario period (**Figure 2**). Hence, QM implicitly assumes that the calibrated correction function and, consequently, intensity-dependent climate model biases are stationary in time. Especially under changing climatic conditions this assumption is uncertain (e.g., (Bellprat, et al., 2013), (Buser, et al., 2009), (Maraun, 2013)). Note, however, that non-stationary biases of simulated mean conditions caused by a systematic shift of the simulated distribution towards conditions subject to different bias characteristics can be meaningful and can in principle be accounted for by QM (Ivanov, et al., 2018). QM evaluations employing pseudo-realities indicate the validity of the calibrated correction functions also in a future climate (Ivanov & Kotlarski, 2017).

Temporal variability and remaining biases: QM is a distribution-based correction approach that does not alter the temporal sequence of the raw climate model output. If climate models have misrepresented temporal variability (e.g., biased inter-annual or day-to-day variability or biased trends), remaining biases in the quantile-mapped output are to be expected (Addor and Seibert 2014). Biases in day-to-day variability can, for instance, arise if large-scale blocking situations and corresponding circulation regimes over Europe are not well represented by the raw model (e.g. Scaife et al. 2010). Furthermore and due to the only approximate nature of the QM correction, the quantile-mapped data can be subject to remaining biases in the calibration period itself even for seasonally averaged values. These remaining biases are typically small but, in the case of the CH2018 scenarios, can for instance lead to a systematic underestimation of the observed summer precipitation amounts. This is the reason why *bias correction* approaches are nowadays often referred to as *bias adjustment*, highlighting the fact that not all model biases are removed by the correction procedure.

Changes of extremes: The QM correction function for high and low quantiles can be subject to large uncertainties that partly arise from sampling issues due to a limited number of values considered for the calibration. Furthermore, the bias of values that lie outside the range of the present-day calibra-

tion period (i.e. new extremes that have not been observed in the present-day climate) is not explicitly considered in QM. In our setup, a constant extrapolation of the biases for the 1st and 99th percentile, respectively, is used (see Chapter 2.2). Other approaches, both parametric and non-parametric, are possible (e.g., Gutjahr and Heinemann 2013, Ivanov and Kotlarski 2017) and might yield different results for changes in extremes. The applicability of QM scenarios for assessing changes in extremes therefore needs to be carefully evaluated, especially for extremes beyond the observed 1st and 99th percentile, respectively.

Modification of raw climate change signals: The application of QM can modify the raw models' mean climate change signal and the simulated trends (Themessl et al. 2012, Maurer and Pierce 2014, Gobiet et al. 2015, Casanueva et al. 2018, Ivanov et al. 2018). In the context of CH2018, this modification is minor in most cases but can be substantial for individual GCM-RCM chains, variables and meteorological stations/regions. Among others, a systematic and topography-controlled modification of the raw models' temperature change signals by several tenths of a degree by QM was discovered which partly modifies the elevation dependency of the warming signal and to some extent represents a statistical artifact (see the CH2018 Technical Report for further details). Also relative precipitation increases in raw model output tend to get amplified by QM, a feature that is directly connected to the positive precipitation bias of many GCM-RCM chains and the additive nature of the QM correction. Note that in the presence of intensity dependent model biases these modifications of the raw climate change signal can be meaningful (Gobiet et al. 2015, Ivanov et al. 2018).

Spatial climate variability: When employed in a downscaling context (here: QM Setups A and C) QM can misrepresent small scale spatial climate variability on short time scales, e.g. at daily scales (Maraun 2013). The reason is its deterministic nature when downscaling from coarse climate model grid cells to local scales and the fact that the predictor information (grid-cell based simulated values) is translated to finer scales without any randomization that could mimic small-scale variance. The associated misrepresentation of spatial climate variability at scales finer than the predictor information (i.e., smaller than a climate model grid cell) is illustrated, for instance, by Maraun (2013). Regarding Setup C (QM to high-resolution grid), a further limitation with respect to spatial climate variability is the observational reference dataset. Its quality depends on the accuracy of the underlying rain-gauge measurements and the capability of the interpolation scheme to reproduce precipitation at ungauged locations. Especially for the observational 2 km precipitation product employed (MeteoSwiss 2016b), the effective resolution expressed in terms of the typical inter-station distance (15 to 20 km) is much larger than the nominal 2 km grid spacing. As a consequence, also the quantile-mapped product does not fully represent spatial climate variability at the 2 km scale.

Local-scale processes and feedbacks: QM is a purely empirical and data-driven approach. If applied in a downscaling context (Setups A and C) it connects coarse-resolution climate model information to local-scale conditions without considering the underlying processes that translate a large-scale signal into its local-scale counterpart. If these processes become modified in a climate change context, QM cannot account for it as the technique completely relies on the stationarity of the correction function that is calibrated in a historical reference period. Examples for such processes active in Alpine terrain are local and regional scale circulation systems (slope and valley winds, Föhn) or elevation-dependent warming signals caused by the snow albedo feedback (Kotlarski et al. 2015, Winter et al. 2017). See also the comprehensive discussion of these issues by Maraun et al. (2017). Regarding elevation-dependent warming, QM-based downscaled projections will furthermore be repre-

sentative for the elevation of the underlying RCM grid cell and not necessarily for the elevation of the target station or high-resolution grid cell.

Inter-variable consistency: The QM approach employed in CH2018 is a uni-variate correction and treats each meteorological variable independently. Therefore, inter-variable consistency in the quantile-mapped products is not given a priori. Previous works have, however, shown that QM generally maintains inter-variable consistency as represented by the raw RCM output and can to some extent even correct for biased relations (Wilcke et al. 2013, Ivanov and Kotlarski 2017, Casanueva et al. 2018). An example of the application of QM in a multi-variate context is shown in the CH2018 Technical Report by means of a heat stress index that is based on temperature and humidity. Nevertheless, the CH2018 QM products can be subject to misrepresented inter-variable relations. An obvious example are individual days on which, for instance, quantile-mapped daily maximum temperature can be lower than quantile-mapped daily mean or daily minimum temperature at specific stations or grid cells. The number of these cases is generally small however.

Spatial representativeness: QM to stations (Setup A) uses the simulated output of the climate model grid cell in which a given station of interest is located as predictor. Similarly, QM to high-resolution grid (Setup C) employs raw RCM data bi-linearly interpolated to the location of a specific high-resolution grid cell. In case of a systematically biased spatial variability of the climate model and, in particular, in case of strong circulation biases, the chosen RCM predictor might not be the most representative one for deriving scenario projections at the station or high-resolution grid cell of interest (Maraun and Widmann 2015). In regions of pronounced topography issues of representativeness can arise, even when systematic climate model biases in spatial variability are absent. This is solely due to the fact that the climate model topography is only a coarse representation of the true topography. A given station, for instance, could be located along the northern rim of a ridgeline, while the overlying climate model grid cell might be located along the southern rim of the coarsened climate model topography and might, hence, be exposed to different circulation types. Also, in the case of elevation-dependent forcings such as the snow albedo feedback a nearby climate model grid cell at similar elevation might be more representative for a given station than the directly overlying grid cell.

Circulation biases: The presence of large-scale circulation biases in the underlying climate models, such as a misrepresented frequency of weather types or a systematic dislocation of major storm tracks, might cause representativeness issues (see above) but could also question the applicability of QM in general (Maraun and Widmann 2018). QM, by definition, corrects for local to regional-scale biases but does not consider the nature of these biases and their possible relation to the large-scale flow regime. Previous works have shown that climate model biases can depend considerably on the large-scale weather type (Addor et al. 2016, Photiadou et al. 2016). Hence, bias-corrected fields might be completely inconsistent with the large-scale flow in the underlying climate model, and bias-corrected fields for a given flow regime might be misrepresented. This potential shortcoming can be expected to especially affect inter-variable relations (see above) and to introduce artifacts in spatial climate change patterns. In the context of CH2018, circulation biases of the employed climate models have not been investigated in detail.

5 Summary and Conclusions

This report presents the bias correction and downscaling approach that is employed for the upcoming CH2018 Swiss climate scenarios. The approach largely relies on empirical quantile mapping (QM), a simple yet versatile method for removing intensity-dependent biases present in raw climate model output. Three QM setups are employed, two of them (QM to stations and QM to high-resolution grid) explicitly include a downscaling component. The resulting products provide transient time series at daily resolution for several meteorological variables and can be directly employed in subsequent climate impact assessments. This explicitly includes applications that refer to absolute thresholds of meteorological variables, such as the analysis of frequency changes of days above or below a certain temperature or precipitation threshold.

A dedicated evaluation of the CH2018 QM implementation reveals a satisfactory performance in the present-day climate in terms of an effective removal of mean model biases. Still, remaining biases might be present for extremes, for daily to interannual climate variability, for small-scale spatial climate variability, for inter-variable relations and to some extent even for seasonal climatologies. Similar to all other downscaling and bias correction methods, QM has a range of potential limitations and might not be applicable to all kinds of climate impact research. These limitations mostly originate from the fact that QM is a purely statistical and data-driven method. It does not incorporate physically-based knowledge on the processes that are responsible for either model biases or for small-scale climate variability beyond the scale resolved by the underlying climate models. These potential limitations are summarized in Chapter 4. They often especially arise in topographically structured terrain where spatial climate variability is large and relevant processes are not or only approximately captured by climate models. Also note that the QM-based scenarios are subject to modeling and emission scenario uncertainties as represented by the projection range of the model ensemble at hand.

As a consequence, users of the QM-based scenarios should properly address the uncertainty sources and should assess the validity of the datasets for each specific application.

Acknowledgment

The present work represents a collaborative effort that was mainly carried out by the author and the co-authors of the study, but that was strongly supported by further persons. This especially concerns the preparation and harmonization of climate model and observational data by Curdin Spirig (C2SM), Jan Rajczak (ETH Zurich/MeteoSwiss) and Urs Beyerle (ETH Zurich). Strong technical support was provided by Felix Maurer and Rebekka Posselt (both MeteoSwiss). Jan Rajczak, Kuno Strassmann (C2SM) and Jonas Bhend (MeteoSwiss) provided extremely useful scientific input. Jan Rajczak provided further useful comments during an internal review of the report. Finally, we thank the entire CH2018 consortium and especially the CH2018 working group on downscaling for their feedback and their suggestions in numerous project meetings and discussions.

References

- Addor, N., Rohrer, M., Furrer, R. and Seibert, J., 2016. Propagation of biases in climate models from the synoptic to the regional scale: Implications for bias adjustment. *Journal of Geophysical Research*, Volume 121.
- Addor, N. and Seibert, J., 2014. Bias correction for hydrological impact studies – beyond the daily perspective. *Hydrological Processes*, 28, 4823-4828.
- Bellprat, O., Kotlarski, S., Lüthi, D. and Schär, C., 2013. Physical constraints for temperature biases in climate models. *Geophysical Research Letters*, 40, 4042-4047.
- Boé, J., Terray, L., Habets, F. and Martin, E., 2007. Statistical and dynamical downscaling of the Seine basin climate for hydro-meteorological studies. *International Journal of Climatology*, 27, 1643-1655.
- Bosshard, T., Kotlarski, S., Ewen, T. and Schär, C., 2011. Spectral representation of the annual cycle in the climate change signal. *Hydrology and Earth System Sciences*, 15, 2777-2788.
- Buser, C. M., Künsch, H. R., Lüthi, D., Wild, M. and Schär, C., 2009. Bayesian multi-model projection of climate: bias assumptions and interannual variability. *Climate Dynamics*, 33, 849-868.
- Casanueva, A., Bedia, J., Herrera, S., Fernández, J. and Gutiérrez, J. M., 2018. Direct and component-wise bias correction of multi-variate climate indices: the percentile adjustment function diagnostic tool. *Climatic Change*, 147, 411-425.
- CH2011, 2011. Swiss Climate Change Scenarios CH2011. Published by C2SM, MeteoSwiss, ETH, NCCR Climate, and OcCC, Zurich, Switzerland, 88 pp. Available from www.ch2011.ch.
- Déqué, M., Rowell, D. P., Lüthi, D., Giorgi, F., Christensen, J.H., Rockel, B., Jacob, D., Kjellström, E., de Castro, M. and van den Hurk, B., 2007. An intercomparison of regional climate simulations for Europe: assessing uncertainties in model projections. *Climatic Change*, 81, 53-70.

- Fowler, H. J., Blenkinskop, S. and Tebaldi, C., 2007. Linking climate change modelling to impacts studies: recent advances in downscaling techniques for hydrological modelling. *International Journal of Climatology*, 27, 1547-1578.
- Gobiet, A., Suklitsch, M. and Heinrich, G., 2015. The effect of empirical-statistical correction of intensity-dependent model errors on the climate change signal. *Hydrology and Earth System Sciences*, 19, 4055-4066.
- Gudmundsson, L., Bremnes, J. B., Haugen, J. E. and Engen-Skaugen, T., 2012. Technical Note: Downscaling RCM precipitation to the station scale using statistical transformations – a comparison of methods. *Hydrology and Earth System Sciences*, 16, 3383-3390.
- Gutiérrez, J. M. et al., 2018. An intercomparison of a large ensemble of statistical downscaling methods over Europe: Results from the VALUE perfect predictor cross-validation experiment. *International Journal of Climatology*, in press.
- Gutjahr, O. and Heinemann, G., 2013. Comparing precipitation bias correction methods for high-resolution regional climate simulations using COSMO-CLM. *Theoretical and Applied Climatology*, 114, 511-529.
- Haylock, M. R. et al., 2008. A European daily high-resolution gridded data set of surface temperature and precipitation for 1950–2006. *Journal of Geophysical Research*, 113, D20119.
- Heger, N., Sanderson, B. M. and Knutti, R., 2015. Improved pattern scaling approaches for the use in climate impact studies. *Geophysical Research Letters*, 42, 3486–3494.
- Isotta, F. et al., 2014. The climate of daily precipitation in the Alps: development and analysis of a high-resolution grid dataset from pan-Alpine rain-gauge data. *International Journal of Climatology*, 34, 1657-1675.
- Ivanov, M. A., Luterbacher, J. and Kotlarski, S., 2018. Climate Model Biases and Modification of the Climate Change Signal by Intensity-Dependent Bias Correction. *Journal of Climate*, in press.
- Ivanov, M. and Kotlarski, S., 2017. Assessing distribution-based climate model bias correction methods over an alpine domain: added value and limitations. *International Journal of Climatology*, 37, 2633-2653.
- Jacob, D. et al., 2014. EURO-CORDEX: new high-resolution climate change projections for European impact research. *Regional Environmental Change*, 14, 563-578.
- Kotlarski, S., Ivanov, M. and Schär, C., 2017. Bias-corrected transient scenarios at the local scale and at daily resolution. *CH2011 Extension Series No. 4*, 21 pp. Available from www.ch2011.ch.
- Kotlarski, S. et al., 2014. Regional climate modeling on European scales: a joint standard evaluation of the EURO-CORDEX RCM ensemble. *Geoscientific Model Development*, 7, 1297-1333.
- Kotlarski, S., Lüthi, D. and Schär, C., 2015. The elevation dependency of 21st century European climate change: an RCM ensemble perspective. *International Journal of Climatology*, 35, 3902-3920.
- Maraun, D., 2013. Bias Correction, Quantile Mapping, and Downscaling: Revisiting the Inflation Issue. *Journal of Climate*, 26, 2137-2143.
- Maraun, D., 2016. Bias Correcting Climate Change Simulations - a Critical Review. *Current Climate Change Reports*, 2, 211-220.
- Maraun, D. et al., 2017. Towards process-informed bias correction of climate change simulations. *Nature Climate Change*, 7, 764-773.
- Maraun, D. et al., 2010. Precipitation downscaling under climate change: Recent developments to bridge the gap between dynamical models and the end user. *Reviews of Geophysics*, 48, RG3003.

- Maraun, D. and Widmann, M., 2015. The representation of location by a regional climate model in complex terrain. *Hydrology and Earth System Sciences*, 19, 3449-3456.
- Maraun, D. and Widmann, M., 2018. *Statistical Downscaling and Bias Correction for Climate Research*. Cambridge University Press.
- Maurer, E. P. and Pierce, D. W., 2014. Bias correction can modify climate model simulated precipitation changes without adverse effect on the ensemble mean. *Hydrology and Earth System Sciences*, 18, 915-925.
- MeteoSwiss, 2016a. *Documentation of MeteoSwiss Grid-Data Products. Daily Mean, Minimum and Maximum Temperature: TabsD, TminD, TmaxD*. MeteoSwiss. Available from https://www.meteoswiss.admin.ch/content/dam/meteoswiss/de/service-und-publikationen/produkt/raeumliche-daten-temperatur/doc/ProdDoc_TabsD.pdf.
- MeteoSwiss, 2016b. *Documentation of MeteoSwiss Grid-Data Products. Daily Precipitation (final analysis): RhiresD*. MeteoSwiss. Available from https://www.meteoswiss.admin.ch/content/dam/meteoswiss/de/service-und-publikationen/produkt/raeumliche-daten-niederschlag/doc/ProdDoc_RhiresD.pdf.
- Monhart, S., Sprigi, C., Bhend, J., Bogner, K. and Schär, C., 2018. Skill of Subseasonal Forecasts in Europe: Effect of Bias Correction and Downscaling Using Surface Observations. *Journal of Geophysical Research: Atmospheres*, in press.
- Moss, R. H. et al., 2010. The next generation of scenarios for climate change research and assessment. *Nature*, 463, 747-756.
- Panofsky, H. A. and Brier, G. W., 1968. *Some Applications of Statistics to Meteorology*. Earth and Mineral Sciences Continuing Education, College of Earth and Mineral Sciences.
- Photiadou, C., Hurk, B., Delden, A. and Weerts, A., 2016. Incorporating circulation statistics in bias correction of GCM ensembles: hydrological application for the Rhine basin. *Climate Dynamics*, 46, 187-203.
- Piani, C., Haerter, J. and Coppola, E., 2010. Statistical bias correction for daily precipitation in regional climate models over Europe. *Theoretical and Applied Climatology*, 99, 187-192.
- Rajczak, J., Kotlarski, S., Salzmann, N. and Schär, C., 2016a. Robust climate scenarios for sites with sparse observations: a two-step bias correction approach. *International Journal of Climatology*, 36, 1226-1243.
- Rajczak, J., Kotlarski, S. and Schär, C., 2016b. Does quantile mapping of simulated precipitation correct for biases in transition probabilities and spelllengths? *Journal of Climate*, 29, 1605-1615.
- Ruosteenoja, K. and Räisänen, P., 2013. Seasonal Changes in Solar Radiation and Relative Humidity in Europe in Response to Global Warming. *Journal of Climate*, 26, 2467-2481.
- Scaife, A. A. et al., 2010. Atmospheric Blocking and Mean Biases in Climate Models. *Journal of Climate*, 23, 6143-6152.
- Sevruk, B., 1997. Regional dependency of precipitation-altitude relationship in the Swiss Alps. *Climatic Change*, 36, 355-369.
- Sherwood, S. C. et al., 2010. Relative humidity changes in a warmer climate. *Journal of Geophysical Research*, 114, D09104.
- Themessl, M., Gobiet, A. and Heinrich, G., 2012. Empirical-statistical downscaling and error correction of regional climate models and its impact on the climate change signal. *Climatic Change*, 112, 449-468.

Themessl, M. J., Gobiet, A. and Leuprecht, A., 2011. Empirical-statistical downscaling and error correction of daily precipitation from regional climate models. *International Journal of Climatology*, 31, 1530-1544.

Wetterhall, F., Pappenberger, F., He, Y., Freer, J. and Cloke, H. L., 2012. Conditioning model output statistics of regional climate model precipitation on circulation patterns. *Nonlinear Processes in Geophysics*, 19, 623-633.

Wilby, R. L. and Dessai, S., 2010. Robust adaptation to climate change. *Weather*, 65, 180-185.

Wilby, R. L. and Fowler, H. J., 2011. Regional Climate Downscaling. In: F. Fung, A. Lopez & M. New: *Modelling the Impact of Climate Change on Water Resources*. Blackwell Publishing Ltd., 34-85.

Wilby, R. L. and Wigley, T. M. L., 2000. Precipitation predictors for downscaling: Observed and general circulation model relationships. *International Journal of Climatology*, 20, 641-661.

Wilcke, R. A., Mendlik, T. and Gobiet, A., 2013. Multi-variable error correction of regional climate models. *Climatic Change*, 120, 871-887.

Winter, K. J.-P. M., Kotlarski, S., Scherrer, S. C. and Schär, C., 2017. The Alpine snow-albedo feedback in regional climate models. *Climate Dynamics*, 48, 1109-1124.

MeteoSchweiz
Operation Center 1
CH-8044 Zürich-Flughafen
T +41 58 460 99 99
www.meteoschweiz.ch

MeteoSvizzera
Via ai Monti 146
CH-6605 Locarno Monti
T +41 58 460 97 77
www.meteosvizzera.ch

MétéoSuisse
7bis, av. de la Paix
CH-1211 Genève 2
T +41 58 460 98 88
www.meteosuisse.ch

MétéoSuisse
Chemin de l'Aérologie
CH-1530 Payerne
T +41 58 460 94 44
www.meteosuisse.ch

